Synthesis of *β*-myrcene / glycidyl methacrylate statistical and amphiphilic diblock copolymers by SG1 nitroxide-mediated controlled radical polymerization

Adrien Métafiot,[†,φ,‡] Jean-François Gérard,[φ] Brigitte Defoort,[‡] and Milan Marić[,†]*

[†]Department of Chemical Engineering, McGill University, 3610 University St., Montreal, H3A 2B2 Quebec, Canada

[φ]Ingénierie des Matériaux Polymères (IMP), CNRS UMR5223, INSA – Lyon, 17 Jean Capelle Avenue, 69621 Villeurbanne, France

[‡]ArianeGroup, 78130 Les Mureaux, France

Keywords: *β*-myrcene; Glycidyl methacrylate; nitroxide-mediated polymerization; copolymerization;

ABSTRACT. Bulk nitroxide-mediated copolymerization (NMP) of β-myrcene (*My*) and glycidyl methacrylate (GMA) with varying GMA molar feed fraction ($f_{GMA,0}$ = 0.10-0.91) was accomplished at 120 °C, initiated by SG1-based alkoxyamine bearing a N-succinimidyl ester group (NHS-BlocBuilder). Low dispersity *My*/GMA copolymers ($Đ < 1.56$) with slight number-average molecular weights (M_n) deviations from predicted values ($M_{n,theo}$ with $M_n/M_{n,theo} > 70$ %) were obtained. The copolymerization was revealed to be statistical, confirmed via Fineman-Ross ($r_{My} = 0.80 \pm 0.31$ and $r_{GMA} = 0.71 \pm 0.15$) and Kelen-Tüdös ($r_{My} = 0.48 \pm 0.12$ and $r_{GMA} = 0.53 \pm 0.18$) approaches. Glass transition temperature (T_g) of the statistical P(*My*-*stat*-GMA)s increased from − 77 °C to + 43 °C as the GMA molar fraction incorporated (F_{GMA}) increased from 0.10 to 0.90. High SG1 chain-end fidelity for *My*-rich and GMA-rich P(*My*-*stat*-GMA)s was assessed by phosphorus nuclear magnetic resonance (^{31}P NMR, SG1 fraction > 69 mol%) and chain-extensions in toluene with *My*, GMA and styrene (S) (monomodal shift in M_n). Lastly, diblock P(*My*-*b*-GMA) was made and treated with morpholine to produce amphiphilic copolymer able to self-organize into micelles.

INTRODUCTION.

Conjugated diene-based elastomers such as natural rubber consisting of *cis*-1,4-isoprene repetitive units and copolymers such as styrene-butadiene rubber exhibit unique and diverse properties. Their significant reversible elongation with low hysteresis combined with low modulus, poor abrasion and chemical resistance make them suitable materials for automobile and aircraft tires, steam hoses, automotive weather-stripping and roofing membranes among others[1,2]. However, the incompatibility of hydrocarbon elastomers with polar entities considerably narrows their potential range of applications. Generally, the addition of functional units to non-polar polymers has been extensively explored in order to use them mainly as coupling agents, adhesives, impact modifiers, highly permeable membranes and compatibilizers, for instance, and thus enhance their service properties[3]. Post-polymerization modification was widely used to prepare functional elastomers. For example, functionalization of poly(3-methylenehepta-1,6-diene) by reacting the pendant vinyl groups with various polar groups via a light-mediated thiol-ene method allowed the synthesis of various functional butadiene-based materials with greater hydrophilicity and tunable glass transition temperatures[4]. An epoxide functionalized poly(isobutylene-*co*-isoprene) derivative was also used to cleanly prepare a specific *exo*-diene, allowing subsequent functionalization by Diels-Alder cycloaddition and/or ring-opening of maleic anhydride adducts. This way, valuable multifunctional materials were achieved such as a graft copolymers with poly(ethylene oxide) (PEO) along with carboxylic acid moieties to name but one[5-7].

The insertion of polar groups in the elastomer can also be achieved directly during the polymerization process, thus simplifying the synthesis route. Although coordination[8,9], anionic[10,11] and cationic[12] polymerizations are typically performed to synthesize polydienes, their

sensitivity to impurities and to the presence of functional groups[8] limits their use for straightforward functionalization of diene-based elastomers by direct polymerization. It is for instance commonly reported that functional groups can coordinate with selective catalysts and poison its activity during coordination polymerizations[12]. An intriguing tool to incorporate polar monomers with dienes is reversible-deactivation radical polymerization (RDRP)[13-17] which is a robust tool for the synthesis of well-tailored complex macromolecular architectures with controlled molecular weights. This technique appears to be well-suited for the synthesis of diene-based elastomers since successful RDRPs of 1,3-conjugated dienes, such as isoprene and butadiene, were comprehensively studied[18-21]. Moreover, RDRP is desirable as a route towards well-defined functional polymers thanks to its great tolerance for functional units of monomers and reaction conditions. Well-defined glycidyl-methacrylate-based polymers were mediated by 2-cyanoprop-2-yl 1-dithionaphthalate (CPDN) RAFT agent and initiated by 2,2'-azobisisobutyronitrile (AIBN) in bulk and in benzene[22].

Among RDRP techniques, nitroxide-mediated polymerization (NMP)[15,16,23] under homogeneous conditions in bulk is one of the easiest systems to implement, requiring only the monomer(s) and the initiator. 2,2,6,6-tetramethylpiperidine-*N*-oxyl (TEMPO) nitroxide as trapping agent and benzoyl peroxide as free radical initiator served as the pioneering bicomponent initiating system used for polymerizing styrenic monomers in bulk[24]. However, the high polymerization temperature needed (T ~ 120-130 °C) when using a TEMPO-mediated system combined with the inability to control effectively monomers other than styrenics[25-27] triggered the development of new alkoxyamine structures. In the late 1990s, the synthesis of alkoxyamine unimolecular initiators like 2,2,5-trimethyl-4-phenyl-3-azahexane-3-oxyl (TIPNO)[18,28] and *N*-*tert*-butyl-*N*-[1-diethylphosphono-(2,2-dimethylpropyl)] nitroxide (DEPN or

SG1)[29] increased the variety of monomers polymerizable by bulk NMP with lower temperatures accessible. TIPNO and its derivatives were used to control effectively homopolymerizations of acrylates such as *tert*-butylacrylate[18,30-32], acrylamides such as *N*,*N*-dimethylacrylamide[32-34] and also 1,3-dienes such as isoprene[30,33,34], which was generally poorly controlled by TEMPO-mediated systems[18]. The NMP of isoprene in bulk using TIPNO was effectively controlled with a dispersity (Đ) lower than 1.20 and a linear relationship between the number-average molecular weight (M_n) and the conversion. Following the successful TIPNO-based NMP of isoprene, statistical copolymerizations of isoprene in bulk with styrenics, acrylates and methacrylates were performed in a controlled manner[18]. Random and block copolymers based on associations of 1,3-dienes with functionalized vinyl monomers using TIPNO were successfully prepared[18,31,35-37].

Well-controlled conjugated 1,3-dienes polymerizations were reported for SG1-mediated NMP as well. Harrisson *et al.* reported the successful NMP of isoprene in bulk at 115 ºC using a range of SG1-based alkoxyamines. Poly(isoprene)s exhibiting low dispersities ($Đ < 1.20$) and experimental M_n close to the predicted one at approximately 40 % conversion were achieved[38]. We reported recently the optimized NMP of *β*-myrcene (*My*)[39], an acyclic monoterpene 1,3-diene, in bulk, initiated by the SG1-based succinimidyl ester-terminated NHS-BlocBuilder[40-42], which was derived from the esterification of BlocBuilder initiator with N-hydroxysuccinimide[43]. Moreover, SG1-type initiators led to the synthesis of well-define poly(acrylate)s[44-45] such as poly(*n*-butyl acrylate) and poly(methacrylate)s like poly(methyl methacrylate)[46-47] as accomplished by Charleux and co-workers. Accordingly, these studies highlighted the ease of NMP based on the second generation of acyclic nitroxides, such as SG1 and TIPNO, to homopolymerize conjugated 1,3-dienes and to copolymerize them with functional monomers.

The copolymerization of ``renewable`` *β*-myrcene with functional monomers has been rarely reported although it could provide a wide latitude of polymer properties. In 1993, Trumbo studied the free radical copolymerization of *β*-myrcene with methyl methacrylate and *p*-fluorostyrene at 65 °C initiated by AIBN, allowing the determination of reactivity ratios[48]. To the best of our knowledge, the controlled/living copolymerization of *β*-myrcene with polar monomers by ionic polymerization or RDRP has never been performed. Taken the versatility and the robustness of NMP based on the second generation alkoxyamines to copolymerize 1,3-dienes with functionalized vinyl monomers into account, the synthesis of functional *β*-myrcene-based copolymers by SG1-mediated NMP appears to be promising.

In the present study, we report on NHS-BlocBuilder-initiated copolymerization of *β*-myrcene (*My*) with glycidyl methacrylate (GMA) in a controlled manner at 120 °C in bulk. Copolymer composition and kinetics were studied according to the molar feed composition of GMA, $f_{GMA,0}$ = 0.10-0.91. The glass transition behavior of the resulting P(*My*-*stat*-GMA) statistical copolymers was explored as well. The active feature of P(*My*-*stat*-GMA)s was assessed by phosphorus nuclear magnetic resonance (^{31}P NMR) and by their ability to initiate a fresh batch of monomer. Lastly, a P(*My*-*b*-GMA) diblock was achieved and modified using morpholine in order to synthesize readily an amphiphilic poly(*β*-myrcene-*block*-2-hydroxy-3-morpholinopropyl methacrylate) P(*My*-*b*-HMPMA) diblock copolymer.

EXPERIMENTAL SECTION.

◘ Materials.

β-Myrcene (*My*, ≥ 90 %), basic alumina (Al_2O_3, Brockmann, Type I, 150 mesh), calcium hydride (CaH_2, 90-95 % reagent grade), 1,4-dioxane (≥ 99 %) and 2-methyltetrahydrofuran (Me-THF, ≥ 99 % anhydrous) were purchased from Sigma-Aldrich and used as received. Toluene (≥ 99 %), methanol (MeOH, ≥ 99 %), tetrahydrofuran (THF, 99.9 % HPLC grade) and morpholine (≥ 99 % ACS reagent) were obtained from Fisher Scientific and used as received. 2-Methyl-2-[*N*-*tert*-butyl-*N*-(1-diethoxyphosphoryl-2,2-dimethylpropyl)-aminoxy]–*N*-propionyloxy-succinimide, also known as NHS-BlocBuilder (NHS-BB), was prepared according to a published method[43] from 2-(*tert*-butyl[1-(diethoxyphosphoryl)-2,2-dimethylpropyl]aminooxy)-2-methylpropionic acid, also known as MAMA-SG1 (BlocBuilder^{TM}, BB, 99 %, purchased from Arkema and used without further purification), *N*-hydroxy-succinimide (NHS, 98 %, purchased from Aldrich and used as received) and *N*,*N'*-dicyclohexylcarbodiimide (DCC, 99 %, purchased from Aldrich and used as received). Styrene (S, 99 %), methyl methacrylate (MMA, 99 %), glycidyl methacrylate (GMA, 97 %), *tert*-butyl acrylate (*t*BuA, 99 %) and maleic anhydride (MA, 99 %) were obtained from Fisher Scientific and were purified by passing through a column of basic alumina mixed with 5 weight % calcium hydride and then stored in a sealed flask under a head of nitrogen in a refrigerator until needed. The deuterated chloroform ($CDCl_3$, 99.8 %) used as a solvent for proton, carbon and phosphorus nuclear magnetic resonance (^1H, ^{13}C and ^{31}P NMR) was obtained from Cambridge Isotopes Laboratory. Diethyl phosphite (98 %) used as internal reference for ^{31}P NMR was purchased from Sigma-Aldrich.

◘ Copolymerization of *β*-myrcene with glycidyl methacrylate by NMP.

All copolymerizations were done in a 10-mL three-necked round-bottom glass flask equipped with a condenser, a thermal well and a magnetic Teflon stir bar. The flask was placed inside a heating mantle and the equipment was put on a magnetic stirrer. All formulations for *My*/GMA copolymerizations are found in Table 2. For every reaction, the initial molar ratio of monomers and NHS-BB was calculated to give a *My*/GMA copolymer sample with target number-average molecular weight $M_{n,theo} = (M_{My}f_{My,0} + M_{GMA}f_{GMA,0}) \times DP = 30$ kg.mol^{-1} at complete overall conversion ($X = 1.0$) with $DP = ([My]_0 + [GMA]_0) / [NHS\text{-}BB]_0$, the average degree of polymerization. A specific formulation for an initial feed composition of GMA ($f_{GMA,0}$) equal to 0.50 is given as an example (experiment *My*/GMA-50, Table 2). NHS-BB (0.144 g, 0.301 mmol), *My* (4.407 g, 32,350 mmol) and previously purified GMA (4.571 g, 32,156 mmol) were added to the reactor and mixing commenced with the stir bar. A thermocouple was inserted through one of the reactor ports via a thermal well and connected to a controller. A mixture of ethylene glycol/reverse osmosis water (30/70 vol%) was circulated via a chilling unit (Fisher Scientific Isotemp 3016D Digital Refrigerated Bath) through the condenser connected to the second neck of the reactor. The chiller was set to 4 ºC. The condenser was capped with a rubber septum with a needle inserted to relieve the pressure of the nitrogen purge applied during the reaction. The third port was sealed with a septum and used as the sampling port. The reactor was sealed and a purge of ultra-pure nitrogen was then introduced to the reactor for 30 min to deoxygenate at room temperature the reactants prior to polymerization. The purge was vented through the reflux condenser. After purging, the reactor was heated at a rate of about 10 °C.min^{-1} to 120 °C with continuous nitrogen purge. The initial polymerization time was taken when the reactor temperature reached 100 ºC. Samples were then taken from the reactor periodically by a

syringe until the end of the experiment or until the samples became too viscous to withdraw. Reaction was then stopped by removing the reactor from the heating mantle and letting the contents cool down to room temperature, while maintaining a nitrogen purge. For each sample withdrawn, the crude polymer was precipitated with excess methanol. The precipitated polymer was dried first under intense air flow for a few hours and then at 50 °C under vacuum in the oven overnight. Nuclear magnetic resonance (NMR) and gel permeation chromatography (GPC) were used to characterize the samples and their specifications are given in the Characterization section. For the specific example cited, the overall conversion was 91.0 % (individual conversions: $X_{My} = 84.2$ % and $X_{GMA} = 94.6\%$) at the end of the experiment ($t = 300$ min) and the molar composition of GMA in the final copolymer was $F_{GMA} = 0.58$ as determined by ^{1}H NMR. The final product exhibited $M_n = 21.9$ kg.mol^{-1} and $Đ = 1.46$ as characterized by GPC. All final *My*/GMA copolymer characteristics can be found in Table 3.

The exact same procedure was followed for *My* homopolymerization as a first step to make P(*My*-*b*-GMA) diblock copolymer (experimental conditions and results in Supporting Information, Table S2) and copolymerizations of *My* with methyl methacrylate (MMA), *tert*-butyl acrylate (*t*BuA) and maleic anhydride (MA). The formulations used for these latter experiments and the features of the final copolymers synthesized are summarized in Table 1.

▫ Chain-extension of poly(*β*-myrcene-*stat*-glycidyl methacrylate) P(*My*-*stat*-GMA) statistical copolymer macroinitiator with *β*-myrcene, glycidyl methacrylate and styrene.

All chain-extensions from P(*My*-*stat*-GMA) macroinitiators were performed in very similar setup to that used for the *My*/GMA copolymerizations with the use of a 25-mL reactor

this time. All formulations can be found in Table 4B. As a brief illustration, the chain-extended product *My*/GMA-22-GMA was synthesized using a statistical P(*My*-*stat*-GMA) copolymer (*My*/GMA-22, $F_{GMA} = 0.22$, $M_n = 11.3$ kg.mol^{-1}, $Đ = 1.27$, 1.011 g, 0.0895 mmol) that was added to the reactor along with toluene (7.615 g), *My* (0.603 g, 4.426 mmol) used as controlling comonomer and previously purified GMA (5.967 g, 42.021 mmol). The reactor was sealed and the contents were mixed and bubbled with nitrogen for 30 min. The mixture was then heated to 110 °C and allowed to react for 60 min while maintaining a nitrogen purge. Samples were drawn periodically via syringe. The samples and the final block copolymer were precipitated in excess methanol and allowed to dry overnight in a vacuum oven at 50 °C. *My*/GMA-22-GMA exhibited $M_n = 29.1$ kg.mol^{-1}, $Đ = 1.49$ and $F_{GMA} = 0.65$. The results of the various chain-extensions from P(*My*-*stat*-GMA) copolymers are given Table 4C. The same procedure was applied for the synthesis of P(*My*-*b*-GMA) diblock copolymer, from P(*My*) macroinitiator, used for the subsequent treatment with morpholine (Supporting Information, Table S2).

▫ Synthesis of poly(*β*-myrcene-*block*-2-hydroxy-3-morpholinopropyl methacrylate) P(*My*-*b*-HMPMA) diblock copolymer.

A conventional reflux apparatus with a 10-mL three-necked round-bottom glass flask was used. NMP-based P(*My*-*b*-GMA) diblock synthesized previously ($F_{My} = 0.58$, $M_n = 23.8$ kg.mol^{-1}, $Đ = 1.89$, 0.210 g, 0.009 mmol, Table S2 in Supporting Information) was dissolved in 2-methyltetrahydrofuran (Me-THF, ~ 5.3 g) and then morpholine (0.330 g, 3.791 mmol, 6.4 eq. relative to GMA repeating units) was added. The reaction medium was vigorously mixed and deoxygenated via N_2 bubbling for 30 min before heating to 77 °C for three hours while

maintaining a gentle nitrogen purge. The final product was precipitated in reversed osmosis water, decanted, filtered via Büchner funnel and the resulting white polymer was dried in a vacuum oven at 50 °C overnight. This post-polymerization treatment yielded P(*My*-*b*-HMPMA) diblock with a complete conversion of the epoxide rings after three hours as determined by ^{1}H NMR. P(*My*-*b*-HMPMA) exhibited $M_n = 26.5$ kg.mol^{-1} and $Đ = 1.91$ as characterized by GPC (Supporting Information, Figure S11). The complete experimental conditions and results can be found in the Supporting Information, Table S2. Dynamic Light Scattering (DLS) was eventually used to measure the hydrodynamic diameter of P(*My*-*b*-HMPMA) particles dispersed in water (**in the range of ??? nm**). **The DSL results are giv**en in the Supporting Information, Table ???.

◘ Characterization.

The (overall) monomer conversion X was determined by proton nuclear magnetic resonance (^{1}H NMR) and calculated from formula 1:

$$\mathbf{X = X_{My} f_{My,0} (+ X_{YY} f_{YY,0})} \quad \mathbf{(1)} \quad \textit{with YY = MMA, GMA, tBuA or MA}$$

where $f_{My,0}$ and $f_{YY,0}$ are the initial molar fractions of *My* and YY respectively and X_{My} and X_{YY} are the individual conversions of *My* and YY respectively. X_{My} and X_{YY} were determined with a Varian NMR Mercury spectrometer (^{1}H NMR, 300 MHz, 32 scans) using $CDCl_3$ deuterated solvent. The signal of the solvent ($\delta = 7.27$ ppm) was used as reference for chemical shifts. *My* conversion was calculated by comparing the integrated peaks corresponding to the aliphatic protons of the monomer ($\delta = 2.15$-2.30 ppm, 4H), the aliphatic protons of the polymer ($\delta =$ 1.90-2.15 ppm, 8H) and the protons of the two methyl groups of both monomer and polymer (δ

= 1.55-1.75 ppm, 6H). MMA conversion was obtained by comparing the integrated peaks corresponding to the vinyl protons of the monomer (δ = 6.10 and 5.55 ppm, 2H) to the methoxy group of the polymer (δ = 3.63 ppm, 3H). GMA conversion was determined using the vinyl protons of the monomer (δ = 6.15 and 5.60 ppm, 2H) and the non-equivalent protons of the methylene bonded to the ester oxygen (δ = 4.20-4.50 and 3.65-4.00 ppm, 2H), the methine proton of the oxirane ring (δ = 3.05-3.30 ppm, 1H) and the non-equivalent protons corresponding to the methylene of the ring (δ = 2.75-2.90 and 2.55-2.70 ppm, 2H) for both the monomer and the polymer. *t*BuA conversion was calculated via the vinyl protons (δ = 5.70 and 6.00 ppm, 2H) and the methyl protons (δ = 1.47 ppm, 9H) of the monomer and the methyl protons of the polymer (δ = 1.42 ppm, 9H). MA conversion was determined by comparing the integrated peaks corresponding to the vinylic protons of the monomer (δ = 7.04 ppm, 2H) to the methine protons of the polymer (δ = 2.90-3.55 ppm, 2H). Styrene (S) conversion when performing chain-extensions was determined using the vinyl protons of the monomer (δ = 6.70-6.80, 5.70-5.80 and 5.20-5.30 ppm, 3H) and the aromatic protons of both monomer and polymer (δ = 6.90-7.50 ppm, 5H). Regarding the post-polymerization treatment of poly(β-myrcene-*block*-glycidyl methacrylate) P(*My*-*b*-GMA) diblock with morpholine, the NMR conversion from GMA repetitive units to 2-hydroxy-3-morpholinopropyl methacrylate HMPMA repetitive units was calculated using the methine proton of the oxirane ring (δ = 3.05-3.30 ppm, 1H) and the non-equivalent protons corresponding to the methylene of the ring (δ = 2.75-2.90 and 2.55-2.70 ppm, 2H) for P(GMA) and the methylene protons attached to the morpholine ring (δ = 3.55-3.80 ppm, 4H and 2.55-2.70 ppm, 4H) and the aliphatic protons neighbor of the tertiary amine (δ = 2.30-2.55 ppm, 2H).

The regioselectivity of the *My* repetitive units in the various *My*-based polymers was determined by using the same spectra (^{1}H NMR, 300 MHz Varian NMR Mercury spectrometer, $CDCl_3$ eluent, 32 scans). Comparing the three integrated peaks at δ = 4.70-4.80 ppm (two vinyl protons of 3,4-addition and two vinyl protons of 1,2-addition), δ = 5.00-5.25 ppm (two olefinic protons of 1,4-addition, one olefinic proton of 1,2-addition and one olefinic proton of 3,4-addition) and δ = 5.30-5.50 ppm (one olefinic proton of 1,2-addition) allowed the three different types of configurations to be quantified[49]. The two stereoisomers of 1,4-P(*My*), *cis*-1,4-P(*My*) and *trans*-1,4-P(*My*), were quantified using ^{13}C NMR (300 MHz Varian NMR Mercury spectrometer, $CDCl_3$ eluent at δ = 77.4 ppm, 1000 scans) chemical shifts of specific nuclei: methylene carbon at δ = 37-38 ppm (*trans*-, 37,6 ppm; *cis*-, 37.1 ppm) and the quaternary carbon at δ = 131-132 ppm (*trans*-, 131.7 ppm; *cis*-, 131.3 ppm)[50]. Deconvolution (Mnova® software, GSD options, 5 fitting cycles with high resolution, proportional line width new spectrum with factor 0.30) was applied to all ^{13}C NMR spectra in order to improve the quality of the integrations.

^{31}P NMR spectroscopy was also performed to determine the molar fraction of two P(*My*-*stat*-GMA)s capped with SG1 moiety. A 5 mm diameter Up NMR tube with 800 scans being performed in a 200 MHz Varian Gemini 2000 spectrometer operating at 81 MHz was used to obtain the spectra. Polymer (mass of polymer = 0.0528 g with M_n = 11.3 kg.mol^{-1} for *My*/GMA-22 and 0.0405 g with M_n = 8.4 kg.mol^{-1} for *My*/GMA-63), diethylphosphite as internal reference (0.0047 g and 0.0052 g respectively) and $CDCl_3$ were added to the NMR tube. In order to know if *My*-based polymers and diethylphosphite have similar relaxation times, *My*/GMA-63 was run under the exact same conditions with only one scan and no dummy scans (ss = 0). A negligible difference (< 2.6 %) in integral values was measured between this spectrum and the standard one

with multiple scans. It was thereby assumed that diethylphosphite and *My*-based polymers with moderate $M_n < 15$ kg.mol^{-1} relax at the same rate.

The number-average molecular weights (M_n) and the dispersities ($Đ = M_w/M_n$) were measured using gel permeation chromatography (GPC, Water Breeze) with HPLC grade tetrahydrofuran (THF) as the mobile phase. A mobile phase flow rate of 0.3 mL.min^{-1} was applied and the GPC was equipped with 3 Waters Styragel® HR columns (HR1 with a molecular weight measurement range of $10^2 – 5 \times 10^3$ g.mol^{-1}, HR2 with a molecular weight measurement range of 5×10^2 - 2×10^4 g.mol^{-1} and HR4 with a molecular weight measurement range of 5×10^3 - 6×10^5 g.mol^{-1}) and a guard column was used. The columns were heated to 40 °C during the analysis. The molecular weights were determined by calibration with linear narrow molecular weight distribution PS standards (PSS Polymer Standards Service GmbH, molecular weights ranging from 682 g.mol^{-1} to 2,520,000 g.mol^{-1}) and the GPC was equipped with a differential refractive index (RI 2414) detector.

Differential scanning calorimetry (DSC, Q2000TM from TA Instruments) was used under N_2 atmosphere to estimate the various glass transition temperatures (T_gs) of P(*My*-*stat*-GMA) statistical copolymers and *My*-rich and GMA-rich diblock copolymers. Indium standard was used to calibrate temperature while heat flow was calibrated via benzoic acid standard. A temperature range from – 90 °C to + 100 °C using three scans per cycle (heat/cool/heat) at a rate of 10 °C.min^{-1} was typically set. For the T_g measurement, only the second heating run was taken into account to eliminate the thermal history. The reported T_gs were calculated using the injection method from the change in slope observed in the DSC traces.

DLS measurements were performed with a Malvern Zetasizer Nano equipped with a 532 nm 50 mW green laser in order to determine Z-average diameter (Z_{ave}). The error is given as the standard deviation from three separate repeats. The samples were prepared by dissolving P(*My*-*b*-HMPMA) diblocks in THF (molecularly dissolved chains) and adding dropwise reversed osmosis water while stirring. The suspension was heated at 50 ºC for 30 min and the THF was then eliminated by dialysis. Specific conditions for each measurement are detailed in the *Results and Discussion* section.

RESULTS AND DISCUSSION.

A) Attempts to copolymerize *β*-myrcene (*My*) with various functional monomers by SG1 nitroxide-mediated copolymerization (NMP).

The insertion of functional groups into poly(*β*-myrcene) P(*My*) elastomer was first tried by nitroxide-mediated copolymerization with various polar monomers. Maleic anhydride (MA), bearing the reactive acid anhydride moiety, was first attempted. Acrylic acid (AA) was not copolymerized due to the sensitivity of the SG1 free nitroxide towards decomposition by strong acids. SG1 can be consumed in degradative side reactions with AA[51]. To avoid this, *tert*-butyl acrylate (*t*BuA), bearing a *tert*-butyl protecting group, was used. The subsequent cleavage after polymerization of the protecting group with trifluoroacetic acid can be performed to yield carboxylic acid groups[52]. Lastly, methyl methacrylate (MMA) was used to see if *My* with a

methacrylate can be done in a controlled manner as has been suggested by isoprene/MMA copolymerizations at quite high MMA content in the initial mixture[18].

The experimental conditions of the various copolymerizations performed and the characterization of the resulting copolymers at the end of the experiments are summarized in Table 1. The complete kinetic study including the semi-logarithmic plot of overall conversion $ln((1-X)^{-1})$ *versus* time, M_n *versus* X plot and Đ *versus* X plot for every experiment is provided in the Supporting Information, Figures S1, S2 and S3.

Table 1. Experimental conditions and results for NHS-BB-initiated copolymerizations of *My* with MA, *t*BuA and MMA monomers.

ID[a]	**[NHS-BB]$_0$ (M)**	**[*My*]$_0$ (M)**	**[YY]$_0$**[b] **(M)**	**Solvent**	**[Solvent]$_0$ (M)**	**T (°C)**	**$M_{n,theo}$ (kg.mol^{-1})**	**X**[c] **(%)**	**M_n**[d] **(kg.mol^{-1})**	**Đ**[d]
My/MA-90	0.015	2.98	0.35	1,4-Dioxane	5.45	107	29.4	46.1	5.5	1.23
My/MA-50	0.017	2.11	2.18	1,4-Dioxane	5.76	108	29.6	58.3	-[e]	-[e]

My/*t*BuA-90	0.020	5.33	0.57	-	-	115	40.0	64.9	16.7	1.31
My/*t*BuA-70	0.019	4.25	1.85	-	-	115	42.9	66.5	10.4	1.19
My/*t*BuA-50	0.021	3.14	3.11	-	-	115	39.3	85.2	6.4	1.25
My/MMA-50	0.028	3.54	3.51	-	-	110	29.8	59.2	8.4	1.24

a) Experimental identification (ID) given by *My*/YY-XX where the letter abbreviation YY refers to the functional comonomer and the number abbreviation XX refers to the rounded % initial molar fraction of *My* in the mixture ($f_{My,0}$).

b) Initial molar concentration of YY = MA, *t*BuA or MMA in the mixture.

c) Overall monomer conversion $X = X_{My}f_{My,0} + X_{YY}f_{YY,0}$ determined by ^1H NMR in $CDCl_3$.

d) M_n and M_w determined by GPC calibrated with PS standards in tetrahydrofuran (THF) at 40 °C.

e) Undetectable polymer peak on the GPC chromatogram.

- ***My*/MA NMP:**

Two *My*/MA copolymerizations in 1,4-dioxane under reflux (T = 107-108 °C) initiated by NHS-BB and with two distinct initial feed composition (*My*/Ma-90 with $f_{My,0}$ = 0.89 and *My*/Ma-50 with $f_{My,0}$ = 0.49) were first performed (Table 1). When adding 10 mol% of MA in the feed, it is of interest to note the early consumption of about one fifth of the monomers at the

commencement of the reaction. Moreover, signification deviations of M_n from the theoretical predictions ($M_n/M_{n,theo} < 0.40$ all along the experiment, Figure S2) suggest the disruption of the NMP process via side reactions. To provide a better insight into the influence of MA on the control of the polymerization, a second reaction was conducted with a stoichiometric initial feed composition of monomers (*My*/MA-50, Table 1). No polymerization occurred as signaled by the absence of polymer peak on the GPC chromatograms and the gravimetric conversion already reached 50 % at $t = 0$ min. The reaction medium turned dark yellow/orange after only 30 minutes and was dark brown at the end of the reaction. These observations suggest a side product was formed at the initial stages of the polymerization, possibly followed by another transformation that was indicated by the colour change. This incompatibility of *My* and MA to copolymerize might be explained by the formation of a Diels-Alder adduct. The Diels-Alder cycloaddition of isoprene with MA to yield 4-methyl-4-cyclohexene-1,2-dicarbocylic anhydride is well-known[53] and a similar mechanism was also reported for the *My*/MA system[54]. Figure S4.a in the supporting information gives the individual *My* and MA conversions versus reaction time for both experiments. Interestingly, a similar trend in consumption for *My* and MA is noticeable regardless the initial feed composition. This supports the assumption of the formation of a cyclic side product from a stoichiometric amount of the monoterpene and the acid anhydride.

- ***My*/*t*BuA NMP:**

The polymerization of acrylates by NMP has become much more facile with second-generation alkoxyamines such as TIPNO and BlocBuilder^{TM}. However, its main challenge is derived from selection of the proper conditions due to their elevated propagation rate constants

(k_p) compared to styrenics. Generally, the consumption of the monomer is significantly faster than the consumption of the initiating alkoxyamine, resulting in a poorly controlled polymerization[25]. *My*/*t*BuA copolymerization, mediated by NHS-BB, was carried out in bulk at 115 °C and targeting about 40 kg.mol^{-1} at X = 100 % (Table 1). An investigation of the influence of the initial feed composition over the control of the polymerization was performed with $f_{My,0}$ = 0.90, 0.70 and 0.50 (experiments *My*/*t*BuA-90, *My*/*t*BuA-70 and *My*/*t*BuA-50 respectively). Regardless the initial feed composition, *t*BuA conversion was higher than *My* conversion (Figure S4.b, Supporting Information) indicating the higher reactivity of this acrylate with a likely predominance of the propagating macro-radical to add *t*BuA monomer, whatever the terminal active unit (---*My** or ---*t*BuA*). Relatively low dispersities lower than 1.40 were obtained, even at high overall conversion X > 60 %, for every experiment (Figure S3). However, attention can be paid to the evolution of the average chain length with respect to $f_{tBuA,0}$. Deviations of experimental M_n from $M_{n,theo}$ were greater as $f_{tBuA,0}$ increased. Although the copolymerization of *My* with 10 mol% of *t*BuA led to a satisfactory control of the NMP with a linear increase of M_n with conversion, the initial addition of 30 and 50 mol% of *t*BuA in the feed affected significantly the kinetics of the reaction. Indeed, experiment *My*/*t*BuA-70 exhibited M_n plateauing very early and remaining constant during the whole reaction and this observation was even more marked for experiment *My*/*t*BuA-50 with higher $f_{tBuA,0}$ (Figure S2). The predominance of chain transfer side reactions due to the presence of *t*BuA, terminating irreversibly the copolymer chains and thus lowering M_n values can be hypothesized. A secondary backbiting reaction, consisting of an intramolecular chain transfer event in which the propagating chain-end radical loops back and abstracts a hydrogen atom on its own backbone, may have occurred. It is now well-established that backbiting occurs during radical polymerization of acrylates, which can lead to propagation

or chain-scission[55-56]. More specifically, backbiting reactions in the presence of *t*BuA leading to the formation of mid-chains radicals was also reported[57-58]. Accordingly, the lack of linearity in the M_n versus X plots for the NMP of *My*/*t*BuA might be due to the occurrence of backbiting reactions, converting chain-end radicals to less reactive mid-chain radicals. With this assumption, the synthesis of branched P(*My*-*co*-*t*BuA) under these reaction conditions is probable. It is also of interest to notice the evolution of the regioselectivity of *My* repetitive units in the P(*My*-*co*-tBuA) copolymers. As $f_{tBuA,0}$ increased, the molar fraction of 1,2-content increased whereas the fraction of 1,4-addition decreased (Figure S5, Supporting Information). While the SG1 nitroxide-mediated homopolymerization of *My* resulted in 1,4-rich-P(*My*) containing a minor proportion of 1,2- and 3,4-contents (< 20%)[39], it appears that 1,2-addition is encouraged due to the presence of *t*BuA likely as terminal or penultimate unit of the propagating species.

- ***My*/MMA NMP:**

Although some exceptions were reported using well-tailored alkoxyamines such as 2,2-diphenyl-3-phenylimino-2,3-dihydroindol-1-yloxyl nitroxide (DPAIO)[59], the simplest way to control effectively the polymerization of methacrylate monomers by SG1-mediated NMP is to use a small concentration of controlling comonomer such as styrene[46,60]. Benoit and coworkers reported the effective control of the bulk NMP of MMA initiated by 2,2,5-trimethyl-3-(1′-phenylethoxy)-4-phenyl-3-azahexane alkoxyamine and using isoprene at about 20 mol% in the feed[18]. In order to know if methacrylates can be readily copolymerized with *My* by NMP, MMA monomer was selected as a reference monomer. A stoichiometric feed composition of monomers

($f_{My,0}$ = 0.50, experiment *My*/MMA-50, Table 1) was heated at 110 °C in the presence of NHS-BB initiator. As shown in Figure S1 by the linear relationship between $ln((1\text{-}X)^{-1})$ versus reaction time t (correlation coefficient $R^2 > 0.98$), a first-order kinetic behavior was observed, assuming a quasi-constant concentration of the active propagating species during the polymerization. Linear trends can be noted regarding individual *My* and MMA conversions with respect to the polymerization time as well (Figure S4.c, Supporting Information). Moreover, M_n values increased linearly with the overall conversion (Figure S2) and narrow molecular weight distributions were obtained ($Đ \leq 1.32$, Figure S3). Consequently, the reversible dynamic equilibrium between the dormant SG1-terminated P(*My*-*co*-MMA) copolymers and active P(*My*-*co*-MMA) radicals was likely established. At $X > 20$ %, non-negligible deviations of the M_n from the predicted ones can be noted yet (Figure S2). This tendency of M_n to plateau at increasingly higher conversions is presumably due to irreversible terminations, commonly observed for copolymerizations of methacrylates using SG1-based alkoxyamine[61-63]. Since the copolymerization was done in bulk, it can be assumed that the side reactions resulted mainly from β-hydrogen transfer to SG1[63] or intramolecular chain transfer[64].

The satisfactory results regarding the SG1 nitroxide-mediated copolymerization of *My* with MMA in bulk prompted us to study more exhaustively the copolymerization of *My* with another methacrylic ester that contains functional groups, such as the epoxy-functional glycidyl methacrylate (GMA).

B) *My*/GMA statistical copolymerization by SG1 NMP.

We reported previously the optimized NMP of *My* (experiment *My*/GMA-100 herein, Tables 2 and 3) performed at 120 °C in bulk and initiated by NHS-BB alkoxyamine, leading to M_n on average 90 % of predicted $M_{n,theo}$, $Đ < 1.3$ and a resulting SG1-capped P(*My*) able to reinitiate cleanly a second batch of styrene[39]. Accordingly, we attempted to copolymerize *My* and GMA, with initial *My* molar feed compositions $f_{My,0}$ = 0.10-0.90, under the same reaction conditions. Notably, well-controlled NMP copolymerizations of isoprene (I) with small amounts of GMA (1-10 wt%) in toluene were also performed at 120 °C in a medium pressure reactor[65]. The formulations for the various *My*/GMA copolymerizations are summarized in Table 2.

▫ **Effect of feed composition on copolymer composition.**

The influence of $f_{My,0}$ over the molar composition of the resulting P(*My-co*-GMA) copolymer was explored at relatively low overall conversion ($X \leq 23.2$ % for every copolymerization). The compositions of the copolymers synthesized (F_{My} and $F_{GMA} = 1 - F_{My}$, Table 3 for the final compositions) during the experiments were determined by ^{1}H NMR (see Experimental Section for full information and Figure S6 in Supporting Information for the spectral assignments of ^{1}H NMR from experiment *My*/GMA-50). It should be noted that the terminal model[66] was used, which assumes that the reactivity of an active center depends only on the nature of the terminal monomer unit of the growing chain.

Table 2. *My*/GMA copolymerization formulations for various compositions at 120 °C in bulk initiated by NHS-BB and targeting $M_{n,theo}$ = 30 kg.mol^{-1} at X = 100 %.

ID[(a)]	[NHS-BB]$_0$ (M)	[*My*]$_0$ (M)	[GMA]$_0$ (M)	$f_{My,0}$	*t* (min)
My/GMA-0	0.036	0	7.52	0	-[(b)]
My/GMA-10	0.034	0.72	6.55	0.10	15
My/GMA-20	0.033	1.43	5.67	0.20	60
My/GMA-30	0.032	2.01	4.86	0.29	90
My/GMA-40	0.031	2.69	4.02	0.40	180
My/GMA-50	0.030	3.26	3.39	0.49	300

My/GMA-60	0.029	3.85	2.54	0.60	300
My/GMA-70	0.029	4.40	1.83	0.71	300
My/GMA-80	0.028	4.85	1.23	0.80	360
My/GMA-90	0.027	5.36	0.61	0.90	300
My/GMA-100[(c)]	0.025	5.61	0	1	420

a) Experimental identification (ID) given by *My*/GMA-XX where the number abbreviation XX refers to the rounded % initial molar fraction of *My* in the mixture ($f_{My,0}$).

b) Experiment stopped before the arbitrary time t = 0 min due to a highly viscous reaction medium.

c) *My* homopolymerization performed previously under the same experimental conditions[39].

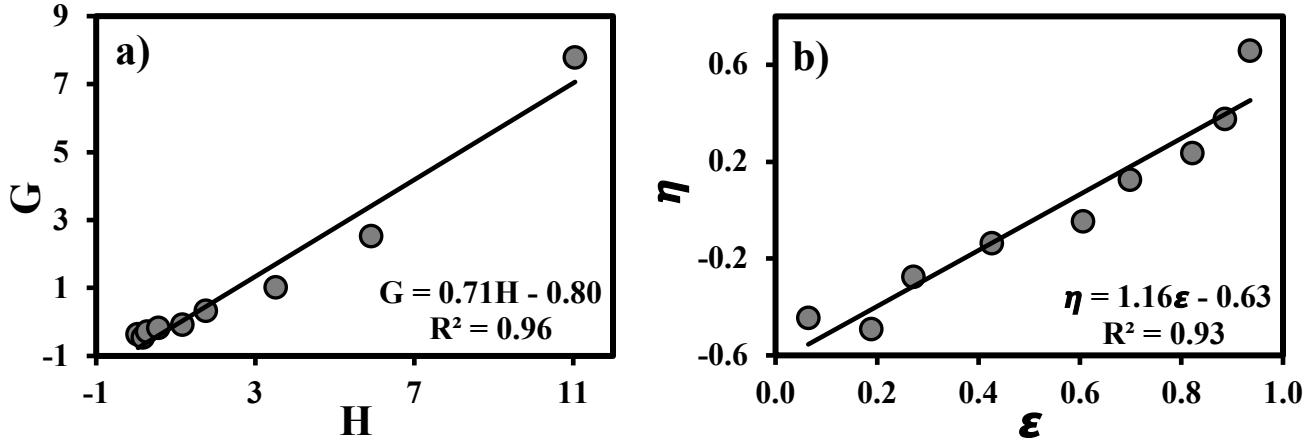

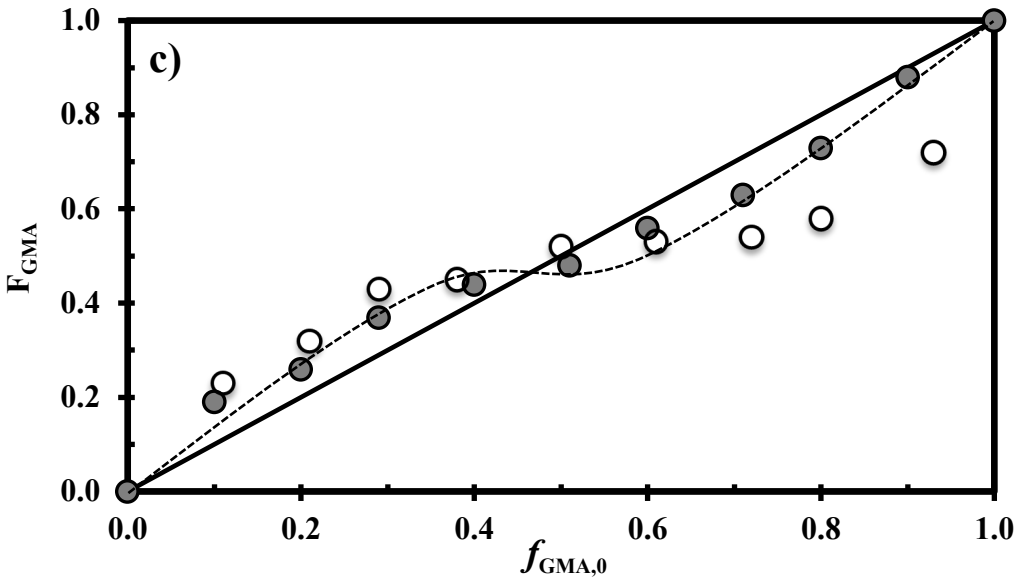

Figure 1. (a) FR and **(b)** KT plots to determine the binary reactivity ratios (solid grey circles (●) corresponding to experimental data while solid lines refer to the trend lines) and **(c)** Mayo−Lewis plot of copolymer composition with respect to GMA (F_{GMA}) versus initial glycidyl methacrylate feed composition $f_{GMA,0}$ (experimental data indicated by the solid grey circles (●) while the dashed line is the associated trend line; open circles (○) refer to the data of Contreras-Lopez and coworkers for the I/GMA system using conventional free radical copolymerization at 70 °C in bulk initiated by benzoyl peroxide[72]; the straight line indicates the azeotropic composition ($f_{GMA,0} = F_{GMA}$)) for *My* and GMA statistical copolymerizations done in bulk at 120 °C using NHS-BB. See Table S1 in the supporting information for the full characterization of the samples used.

Table S1 in the supporting information contains experimental data used to estimate the monomer reactivity ratios for low-conversion P(*My-co*-GMA)s via the Fineman-Ross (FR)[67] and

the Kelen-Tudos (KT)[68] approaches (equations used for the calculation of the reactivity rations can be found in the supporting information, page S6). Figures 1.a and 1.b show the plots of the parameters for both linear methods, yielding $r_{My} = 0.80 \pm 0.31$ and $r_{GMA} = 0.71 \pm 0.15$ ($r_{My} \times r_{GMA} = 0.57 \pm 0.27$) via the FR approach and $r_{My} = 0.48 \pm 0.12$ and $r_{GMA} = 0.53 \pm 0.18$ ($r_{My} \times r_{GMA} = 0.25 \pm 0.17$) using the KT formula. The errors associated with the experimental data were derived from the standard errors of the slopes from FR and KT plots. Tidwell and Mortimer[69] highlighted the defects of the linear methods and suggested the use of a non-linear least-squares (NLLS) procedure. Therefore, the non-linear least-squares fitting to the data was also used to determine the reactivity ratios (Supporting Information, page S6). Since a starting point needs to be provided, the reactivity ratios calculated by the KT method were used as initial guesses. NLLS procedure applied to the Mayo-Lewis equation[70] showed good agreement with the other methods employed in this study, with $r_{My} = 0.49 \pm 0.13$ and $r_{GMA} = 0.50 \pm 0.13$ with 95 % confidence bounds. Regardless the method applied, $r_{My} < 1$ and $r_{GMA} < 1$ pointing out the preference of --*My*$^{\bullet}$ and --GMA$^{\bullet}$ propagating species for adding the other monomer (GMA and *My* respectively) and each of these propagation steps proceed at a similar rate since $r_{My} \approx r_{GMA}$. Interestingly, $0.25 \leq r_{My}\, r_{GMA} \leq 0.57$ indicating that the behavior of *My*/GMA system cannot be considered as an ideal copolymerization ($r_{My}\, r_{GMA} = 1$, the relative rates of incorporation of the two monomers into the copolymer are independent of the identity of the unit at the end of the propagating species). As the product of the reactivity ratios decreases from one toward zero, there is an increasing tendency toward alternation, where each of the two types of propagating species preferentially adds the other monomer. Since $r_{My}\, r_{GMA} \geq 0.25$ is relatively far from zero, the predominance of the statistical placement over alternating arrangement of *My* and GMA monomers along the copolymer chain can be assumed. Other diene/GMA were copolymerized

by conventional free radical polymerization. P(I-*stat*-GMA) statistical copolymers were synthesized by benzoyl peroxide-initiated free radical polymerization in bulk at 80 °C and $r_I = 0.195 \pm 0.005$ and $r_{GMA} = 0.135 \pm 0.005$ were determined graphically[71]. More recently, Contreras-López and coworkers reported $r_I = 0.119 \pm 0.048$ and $r_{GMA} = 0.248 \pm 0.161$, via the nonlinear method of Tidwell-Mortimer with 95 % confidence intervals, for I/GMA copolymerization in bulk at 70 °C initiated by benzoyl peroxide[72]. Accordingly, lower reactivity ratios were calculated for I/GMA system with $r_I\, r_{GMA}$ less than 0.03 indicating the stronger tendency to alternate compared to *My*/GMA system polymerized by bulk NMP at 120 °C. Two parameters may explain the difference in constants observed: the significantly higher reaction temperature for *My*/GMA copolymerization (120 °C) and the nature of the conjugated 1,3-diene and thus the effect of the lateral C6/C8 side group borne by *My* units.

Figure 1.c shows the curve of instantaneous copolymer composition (mole fraction of GMA) obtained for a given feed monomer composition regarding the *My*/GMA system as well as I/GMA system studied by Contreras-López *et al.*[72]. A similar dependence of F_{GMA} over $f_{GMA,0}$ can be noted for both systems with GMA-rich instantaneous copolymers produced at $f_{GMA,0} \lesssim 0.45$ and diene-rich instantaneous copolymers formed at $f_{GMA,0} \gtrsim 0.55$. The Mayo-Lewis plot exhibits an azeotropic point at $f_{GMA,0} = 0.47$ for *My*/GMA system where the instantaneous composition of the copolymer is equal to the composition of the monomer feed. The greater deviations observed from the azeotropic composition for the I/GMA copolymerization were due to the lower reactivity ratios and thus the higher rates of cross-propagation measured.

Table 3. Molecular characterization and *My* selectivity at the end of the experiments and kinetic data of P(*My*-*stat*-GMA) copolymers at 120 °C in bulk initiated by NHS-BB and targeting $M_{n,theo} = 30$ kg.mol^{-1} at $X = 1.0$.

ID	F_{My}[a]	X_{My}[b] (%)	X_{GMA}[b] (%)	X[b] (%)	M_n[c] (kg.mol^{-1})	Đ[c]	$\langle k_p \rangle \langle K \rangle$[d] ($10^5$ s^{-1})	1,4-content[e] (%)	1,2-content[e] (%)
My/GMA-0[f]	0	0	-	-	-	-	-	-	-
My/GMA-10	0.05	93.1	79.3	80.7	20.6	1.52	157.0 ± 0.9	47.3	39.2
My/GMA-20	0.16	98.9	86.1	88.7	21.9	1.51	47.7 ± 0.5	48.0	44.9
My/GMA-30	0.21	93.2	82.8	85.9	19.1	1.47	37.6 ± 0.3	58.8	38.1
My/GMA-40	0.34	88.3	92.2	90.6	20.0	1.55	31.2 ± 0.5	61.2	36.5
My/GMA-50	0.42	84.2	94.6	89.4	21.9	1.45	13.3 ± 0.8	69.4	26.5
My/GMA-60	0.57	85.9	93.8	89.1	20.1	1.34	15.1 ± 0.4	64.9	29.6

My/GMA-70	0.67	74.2	91.3	79.3	18.4	1.26	11.4 ± 0.3	70.0	23.1
My/GMA-80	0.78	78.2	95.8	81.7	20.3	1.30	8.2 ± 0.2	74.3	18.2
My/GMA-90	0.89	79.3	96.7	81.0	21.1	1.35	9.1 ± 0.2	81.0	10.5
My/GMA-100[g]	1	66.0	0	40.0	14.9	1.26	4.3 ± 0.7	80.3	9.3

a) Molar fraction of *My* in the copolymer (F_{My}) as determined by ^{1}H NMR in $CDCl_3$ (Figure S6 in Supporting Information for the spectral assignments).

b) Individual monomer conversions X_{My} and X_{GMA} determined by ^{1}H NMR. Average monomer conversion $X = X_{My} f_{My,0} + X_{GMA} f_{GMA,0}$ (further details in the experimental section).

c) M_n and M_w determined by GPC calibrated with PS standards in THF at 40 °C.

d) $\langle k_p \rangle \langle K \rangle$ corresponding to the product of the average propagation rate constant $\langle k_p \rangle$ and the average equilibrium constant $\langle K \rangle$ derived from the slopes $\langle k_p \rangle [P\bullet]$ ([P•] = concentration of propagating macroradicals) taken from the semilogarithmic kinetic plots of $ln((1-X)^{-1})$ versus time in the linear region generally from 0 to 65 min (0 to 30 min for *My*/GMA-30, 0 to 15 min for *My*/GMA-20, 0 to 10 min for *My*/GMA-10, 0 to 120 min for *My*/GMA-100 ; squared linear regression coefficient = $R^2 \geq 0.98$ for every experiment). $\langle k_p \rangle \langle K \rangle$'s estimated from $\langle k_p \rangle [P\bullet]$ and $r = [SG1]_0/[NHS\text{-}BB]_0$ (equation 4). Error bars derived from the standard errors in the slope from the linear fits of $ln((1-X)^{-1})$ versus time.

(e) Regioselectivity determined by ^{1}H NMR in $CDCl_3$. 3,4-content % not mentioned and calculated as follows: 3,4-content% = 100 − 1,4-content% − 1,2-content% (Figure S6 in Supporting Information for further details).

(f) No kinetic study led due to the very early ``caking`` (high viscosity) of the reaction medium.

(g) Results from *My* homopolymerization performed previously under the same experimental conditions[39].

◘ Effect of feed composition on kinetics.

It is of interest to know if *My* and GMA monomers are generally more or less reactive in copolymerization than indicated by their respective rate of homopolymerization. A change in monomer reactivity can influence the final microstructure of the polymer and thus its properties. Even though kinetic data regarding *My* polymerization are scarce, isoprene (I) can be chosen as a reference conjugated 1,3-diene. The propagation rate constant of free radical polymerization of I ($k_{p,I}$) in bulk initiated by di-*tert*-butyl peroxide under irradiation at 5 ºC was estimated at 125 ± 30 L.mol^{-1}.s^{-1} [73]. $k_{p,I} = 50$ L.mol^{-1}.s^{-1} was calculated by Morton *et al.* for the emulsion polymerization of I at 60°C with diisopropylbenzene monohydroperoxide / tetraethylene pentamine (DIBHP/TEPA) catalyst system[74]. On the other hand, $k_{p,GMA}$ for the free radical polymerization of GMA at 50 ºC was estimated through pulsed laser polymerization (1 230 L.mol^{-1}.s^{-1})[75] and through quantum chemistry simulations (1 010 L.mol^{-1}.s^{-1})[76]. Consequently, it can be argued that GMA polymerizes at a rate of about ten times faster than *My* via a radical process.

The semi-logarithmic kinetic plots of $ln((1 - X)^{-1})$ (X = overall conversion) *versus* reaction time are illustrated in Figure 2. The linear trend seen for every *My*/GMA copolymerization until the end of the experiment (squared linear regression coefficient = $R^2 \geq 0.95$) indicates the first-order kinetic behavior of the polymerizations, as described by Equation 1.

$$ln([M]_0 / [M]_t) = ln([M]_0 / ([M]_0(1-X))) = \langle k_p \rangle \times [P^\bullet] \times time \qquad \textbf{(1)}$$

In Equation 1, $[M]_0$ and $[M]_t$ are the concentrations of monomers at time zero and subsequent later time t, respectively, $\langle k_p \rangle$ is the average propagation rate constant and $[P^\bullet]$ is

the concentration of propagating macro-radicals. Regardless *My*/GMA initial feed composition, at the early stages of the copolymerization (caption (d) in Table 3), the straight kinetic trends of the semi-logarithmic plots highlight the lack of irreversible termination reactions so that [P•] was nearly constant. The occurrence of the persistent radical effect (PRE)[25] allowing the reversible entrapment of the propagating radicals by the controlling SG1• nitroxide can be assumed. As expected for the NMP process, this particular kinetic feature can be explained by the homolytic decomposition of NHS-BB alkoxyamine into the propagating alkyl radical and the persistent radical SG1•, allowing the establishment of a dynamic equilibrium between a low concentration of active propagating chains and a predominant concentration of SG1-capped dormant chains. These latter are unable to propagate or terminate, allowing thus the controlled growth of the macro-radicals. It should be noted that deviations from the linear trend can be observed at the last stages of copolymerization, mostly for experiments *My*/GMA-40, *My*/GMA-50 and *My*/GMA-60 (Figure 2a). A decrease in [P•], which might result from irreversible termination reactions increasing the concentration of the persistent radical, could lead to the downward curvature trend seen for these reactions.

$ln((1 - X)^{-1})$ *versus* time plot in the linear region allows the determination of the apparent rate constant, which can be defined as the product of the average propagation rate constant $\langle k_p \rangle$ with the concentration of propagating macro-radicals [P•], $\langle k_p \rangle$[P•]. The apparent rate constant can be related to the average equilibrium constant <K> as the product $\langle k_p \rangle$ <K> by making some assumptions regarding the equilibrium between dormant and active chains. It should be noted that an average propagation rate constant and average equilibrium constant were used since a statistical copolymerization is studied, consisting of a diene and a methacrylate, which likely have very different individual equilibrium constants.

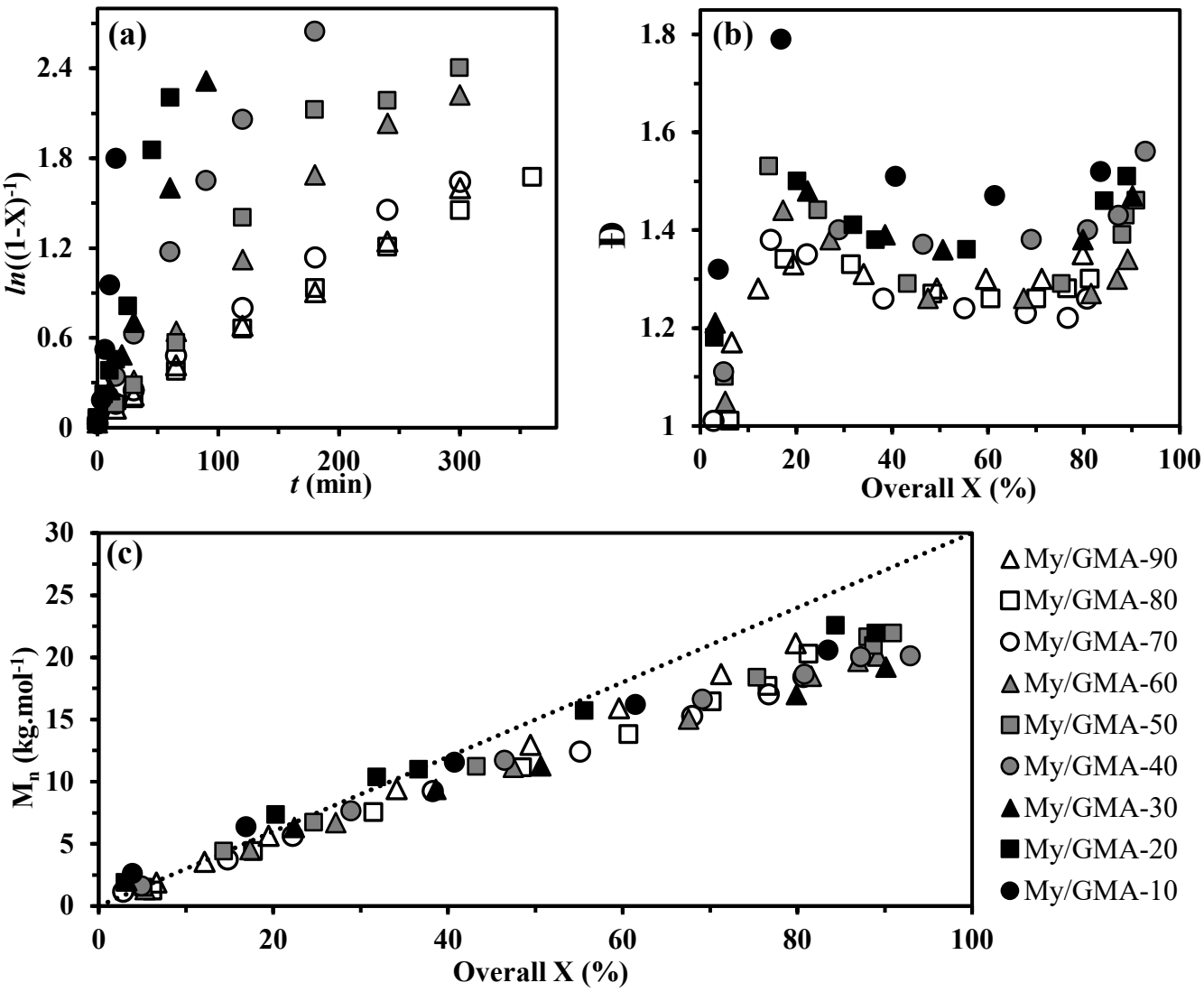
(a)
ln((1-X)^-1)
t (min)
(b)
Đ
Overall X (%)
(c)
M_n (kg.mol^-1)
Overall X (%)
My/GMA-90
My/GMA-80
My/GMA-70
My/GMA-60
My/GMA-50
My/GMA-40
My/GMA-30
My/GMA-20
My/GMA-10

Let

The <K> is defined in terms of the [P•], the concentration of free nitroxide [N•] and the concentration of dormant alkoxyamine terminated species [P-N], as shown in Equation 2.

$$<K> = ([P^{\bullet}] \times [N^{\bullet}]) / [P\text{-}N] \qquad \textbf{(2)}$$

The overall polymerization rate can be defined by the rate of chain propagation which is given by Equation 3.

$$R_p = -\, d[M]/dt = <k_p>[P^{\bullet}][M] \qquad \textbf{(3)}$$

By assuming that the initial concentration of nitroxide $[N]_0$ is high so that $[N] = [N]_0$ in the early stages of polymerization and that [P-N] is approximately equal to the initial concentration of initiator ($[P\text{-}N] = [NHS\text{-}BB]_0$), the following equation 4 can be obtained from Equation 2 with $r = [N]_0/[NHS\text{-}BB]_0$:

$$<k_p><K> \cong (<k_p> \times [P^{\bullet}] \times [N^{\bullet}]_0) / [NHS\text{-}BB]_0 = k_p \times [P^{\bullet}] \times r \qquad \textbf{(4)}$$

Figure 2. (a) Semi-logarithmic kinetic plots of $ln((1-X)^{-1})$ (X = overall conversion) *versus* polymerization time *t*, **(b)** Đ *versus* overall conversion X and **(c)** M_n determined by GPC relative to PS standards in THF at 40 °C for *versus* overall conversion X for the various *My*/GMA copolymerizations in bulk at 120 °C initiated by NHS-BB. The dotted line indicates the theoretical M_n *versus* overall conversion based on the monomer to initiator ratio ($M_{n,theo}$ = 30 kg.mol^{-1} at X = 100 % for every experiment). All experimental ID and characterization of experiments are listed in Table 2 and Table 3. The same legend at the bottom right of the figure is used for each of the three plots.

The reported $<k_p><K>$ in Table 3 were measured during the early stages of the copolymerization, at low or moderate final conversion (X ≤ 45.2 %) except for experiments *My*/GMA-40 and *My*/GMA-10 where the final overall conversions were 67 % and 57 %, respectively. In any case, a linear growth of M_n versus X was observed (Figure 2c), making Equation 4 applicable. As $f_{GMA,0}$ increased, the $<k_p><K>$'s increased with $<k_p><K> = (9.1 \pm 0.2)\ 10^{-5}\ s^{-1}$ at $f_{GMA,0} = 0.10$ to $<k_p><K> = (157.0 \pm 0.9)\ 10^{-5}\ s^{-1}$ at $f_{GMA,0} = 0.90$ (Table 3). These kinetic values are not surprising since k_pK of pure *My* under identical reaction conditions was estimated at $(4.3 \pm 0.7)\ 10^{-5}\ s^{-1}$ [39] while $<k_p><K> = (66 \pm 4)\ 10^{-5}\ s^{-1}$ was measured for GMA/S copolymerization with $f_{GMA,0} = 0.94$ initiated by NHS-BB at 90 °C in 50 wt% 1,4-dioxane solution[40]. The presumable large difference in the k_p between *My* ($k_{p,I} \sim 10^2$ L.mol^{-1}.s^{-1} for isoprene, a structurally similar 1,3-diene[73,74]) and GMA ($k_{p,GMA} \sim 10^3$ L.mol^{-1}.s^{-1} [75,76]), as discussed above, can partly explain the $<k_p><K>$ increase with $f_{GMA,0}$ even though the contribution of the two individual activation-deactivation equilibrium constants cannot be neglected. The higher $<k_p><K>$ values determined when using methacrylate-richer initial feeds agrees with previous studies, reporting similar kinetic trends for the *tert*-butyl methacrylate/S copolymerization at 90 °C in bulk initiated by BlocBuilder™ [77], the GMA/S copolymerization at 90 °C in 1,4-dioxane initiated by NHS-BB[40] and the MMA/S binary system initiated by BlocBuilder™ in bulk at 90 °C [60].

A well-controlled RDRP exhibits linear M_n versus X and low dispersity with monomodal distributions. The general increase in $<k_p><K>$ as a function of increasing $f_{GMA,0}$ suggested the polymerizations were becoming less controlled. This was reflected in faster polymerization rates (Table 3) and higher Đ as shown in Figure 2b. While relatively low dispersities (Đ ≤ 1.38) were measured for *My*-rich initial feed composition ($f_{GMA,0} \leq 0.29$), higher Đ values mainly ranging

from 1.25 to 1.50 were obtained for experiments *My*/GMA-40, *My*/GMA-50 and *My*/GMA-60 with $f_{GMA,0}$ = 0.40-0.60. This tendency was amplified for GMA-rich feeds with broader molecular weight distributions measured, with values typically between 1.35 and 1.55 (Figure 2b). Independently of the initial molar composition, similar Đ versus X trends can be observed. Disregarding the first inaccurate Đ values for X < 10 % (likely underestimation of the dispersity due to the low intensity of the polymer peaks on the GPC chromatograms), Đ was quite elevated at the commencement of the copolymerization (X ~ 15-25 %) but became gradually lower as the overall conversion increased (X ~ 25-70 %). It can be assumed that the dynamic equilibrium between the propagating macro-radicals and the dormant SG1-terminated species was not being established sufficiently at the early stages of the polymerization for the persistent radical effect to be present. At the last stages of the copolymerization (X ~ 70-95 %), a broadening of the molecular weight distribution was apparent for every *My*/GMA experiment, probably underscoring the greater prevalence of termination reactions, resulting in a loss of the SG1 functionality on the chain end. Since a solvent free process was applied, it may be hypothesized that many of the irreversible terminations occurring resulted from β-hydrogen transfer (disproportionation) from propagating P(*My*-*stat*-GMA) radical to SG1[63,78] or intramolecular chain transfer to polymer[64,78].

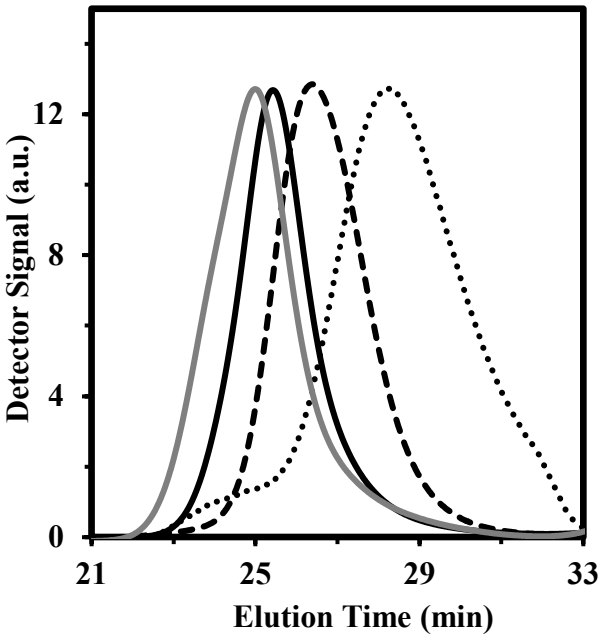

Figure 2c gives M_n versus X for the various experiments. It should be first noted that M_n values have to be carefully compared to the theoretical ones since all GPC measurements were performed using linear poly(styrene) standards, which might not be very accurate for P(*My*-*stat*-GMA) samples. A similar linear growth of degree of polymerization with overall conversion for every *My*/GMA copolymerization with M_n = 18.4-21.9 kg.mol^{-1} at X > 80 % can be seen (Figure 2c). This can be explained by the active feature of the macro-radical chain end for a prolonged period of time, presumably due to the relatively low average equilibrium constant <K> obtained when polymerizing GMA with *My*. M_n values started slightly

Figure 3. Normalized GPC traces of P(*My*-*stat*-GMA) with $f_{GMA,0}$ = 0.51, initiated by NHS-BB at 120 °C in bulk targeting $M_{n,theo}$ = 30 kg.mol^{-1} at quantitative conversion (experiment *My*/GMA-50). The black dotted line, the black dashed line, the black solid line and the grey solid line (from right to left) correspond respectively to the GPC chromatograms of samples taken at 15, 65, 120 and 300 min.

plateauing at X ~ 40 % and non-negligible deviations from the predicted line can be observed at the final stages of the copolymerizations ($M_n/M_{n,theo}$ = 71-88 % at the end of the experiments, Table 3). It may be due to the occurrence of irreversible termination reactions, which were non-longer retarded at X > 40 %.

The GPC traces for experiment *My*/GMA-50 exhibiting a nearly stoichiometric initial feed composition are shown in Figure 3. A monomodal shift of the GPC chromatograms can be observed with a slight tail at longer elution times, most likely resulting from irreversible termination reactions generating low M_n P(*My*-*stat*-GMA) chains. At *t* = 15 min, a minor population of longer chains was detectable at relatively short elution times (23-26 min, Figure 3). As discussed in a previous study reporting the NMP of *My*[39], it may be caused by *My* autoinitiation[79], generating an excess of P• and a fast autopolymerization which makes the mediation by SG1 difficult. This second peak was easily detectable at the commencement of *My*-rich feed copolymerizations ($f_{My,0}$ = 0.60 – 0.90) and hardly noticeable for experiments with higher $f_{GMA,0}$. This tends to confirm that this minor fraction of polymer consisted of high M_n P(*My*) chains resulting from *My* autopolymerization.

Lastly, the influence of $f_{GMA,0}$ over the regioselectivity of *My* units in the final copolymer can be discussed (see Figure S6 in Supporting Information for the determination of 1,2-,3,4- and 1,4-motif for experiment *My*/GMA-50). As already mentioned for *My*/*t*BuA system above, the molar fraction of 1,2-addition increased and that of 1,4-addition decreased with $f_{GMA,0}$ (and thus F_{GMA}). While *My* NMP produced P(*My*) exhibiting a large predominance of 1,4-content (~ 80 mol%) with a minor proportion of 1,2-units (< 10 mol%, experiment *My*/GMA-100, Table 3), the initial addition of 50 mol% of GMA resulted in P(*My*-*stat*-GMA) more than three times richer in 1,2-addition (28.5 mol%, experiment *My*/GMA-50, Table 3). For rich-GMA feeds

($f_{GMA,0}$ = 0.71-0.90), the fraction of 1,2-content exhibited by the final copolymers was around 40 mol%. This change in regioselectivity for *My* units was likely due to the presence of GMA as a terminal or penultimate unit, which might bring about either steric hindrance or electronic effects.

◘ Active feature of *My*-rich and GMA-rich P(*My*-*stat*-S) copolymers.

A paramount feature of a NMP-based polymer is its ability to form a block copolymer via the re-activation of the dormant chains capped by the nitroxide group. Two extra statistical P(*My*-*stat*-GMA) copolymers were synthesized under the same previous experimental conditions (*My*/GMA-37 with $F_{My,1}$ = 0.37 and *My*/GMA-78 with $F_{My,1}$ = 0.78, Table 4A) in order to deem their degree of the active groups, in other words, the fraction of SG1-terminated P(*My*-*stat*-GMA) chains. Several strategies can be adopted to demonstrate whether a SG1-mediated (co)polymer is significantly active enough to re-initiate a second block.

Phosphorus nuclear magnetic resonance (^{31}P NMR) was first used to probe the chain end fidelity of the synthesized *My*/GMA copolymers. This quantitative approach allows to determine the living chain fraction (LF) by detecting the phosphorus-containing SG1 nitroxide end group with diethyl phosphite as an internal reference[46] (see Experimental Section for further details). LF values for *My*-rich (*My*/GMA-78) and GMA-rich (*My*/GMA-37) macroinitiators were 82 ± 5 % and 71 ± 7 %, respectively (Table 4A, standard deviation derived from the difference in macroinitiator M_n value obtained from PS calibration and PMMA calibration, ^{31}P spectra in Supporting Information, Figure S7 and S8), indicating a satisfactory retention of the SG1

fragment. The lower ``living`` fraction exhibited by *My*/GMA-37 can be mainly attributed to the faster NMP performed ($<k_p><K> \sim 40.10^{-5}$ s^{-1} for *My*/GMA-30 with $f_{GMA,0} = 0.70$, Table 3) and thus the more difficult mediation of the binary system, as witnessed by the broader molecular weight distribution ($D_1 = 1.39$), compared to *My*-rich NMP. Generally, these spectroscopic results are a clear indication of the active character of NMP-based P(*My*-*stat*-GMA) copolymers, which may allow efficient chain-extension to produce well-defined block copolymers.

Table 4. Chain-extensions of **A)** *My*-rich and GMA-rich P(*My*-*stat*-GMA) macroinitiators with **B)** *My*, GMA and S monomers in 50 wt% toluene and **C)** molecular characterization of the resulting chain-extended products.

A. Macroinitiator[(a)]							
ID	$f_{My,0}$	$F_{My,1}$	**LF[(b)] (%)**	**X_1 (%)**	**$M_{n,1}$ (kg.mol^{-1})**	**$M_{n,theo,X1}$[(c)] (kg.mol^{-1})**	**$Đ_1$**
My/GMA-37	0.30	0.37	71 ± 7	32.9	8.6	9.9	1.39
My/GMA-78	0.80	0.78	82 ± 5	51.7	11.3	15.5	1.27

B. Formulation of chain-extension								
ID	**[Macro-initiator]$_0$ (M)**	**[*My*]$_0$ (M)**	**[GMA]$_0$ (M)**	**[S]$_0$ (M)**	**[Toluene]$_0$ (M)**	**$M_{n,theo}$[(d)] (kg.mol^{-1})**	**T (^{o}C)**	***t*** **(min)**
My/GMA-37-*My*	0.005	2.741	0	0	4.536	81.9	120	260
My/GMA-37-S	0.005	0	0	3.827	4.807	82.9	110	90
My/GMA-78-GMA/*My*	0.005	0.259	2.612	0	5.081	85.6	110	60
My/GMA-78-S	0.006	0	0	3.660	4.813	80.5	110	100

C. Chain-extended copolymer[(a)]						
ID	**X_2 (%)**	**$F_{My,2}$**	**$F_{S,2}$**	**$M_{n,2}$ (kg.mol^{-1})**	**$M_{n,theo,X2}$[(e)] (kg.mol^{-1})**	**$Đ_2$**
My/GMA-37-*My*	45.3	0.84	0	29.2	41.8	1.85
My/GMA-37-S	37.1	0.06	0.81	35.4	36.2	1.46

My/GMA-78-GMA/*My*	30.8	0.35	0	29.1	34.2	1.50
My/GMA-78-S	26.9	0.24	0.70	28.4	29.9	1.36

a) The indexes "1" and "2" refer respectively to the final features of the P(*My*-*stat*-GMA) macroinitiator and the whole chain-extended diblock copolymer (macroinitiator + P(*My*), P(GMA) or PS segment added).

b) LF corresponds to the living molar fraction of macroinitiator chains terminated by a SG1 unit and was measured by ^{31}P NMR in $CDCl_3$ (Figures S7 and S8 in Supporting Information for ^{31}P NMR spectra).

c) $M_{n,theo,X1}$ corresponds to the predicted $M_{n,1}$ at the respective X_1 measured experimentally and was calculated as follows: $M_{n,theo,X1} = (X_1 / 100)\, M_{n,theo,1}$ with $M_{n,theo,1} = 30$ kg.mol^{-1} at X = 100 %.

d) $M_{n,theo}$ corresponds to the targeted number-average molecular weight of the whole chain-extended diblock copolymer (macroinitiator block + extended block) at X = 100 %.

e) $M_{n,theo,X2}$ corresponds to the predicted $M_{n,2}$ of the whole chain-extended diblock copolymer (macroinitiator block + second block added) at the respective X_2 measured experimentally and was calculated as follows: $M_{n,theo,X2} = (X_2 /100)\,(M_{n,theo} - M_{n,1}) + M_{n,1}$ (= Predicted M_n of the second block added at conversion X_2 + experimental M_n of the macroinitiator).

To confirm the ^{31}P NMR quantitative analysis, *My*/GMA-78 and *My*/GMA-37 were used as macroinitiators in the polymerization of *My*, GMA and styrene (S) in 50 wt% toluene solution at T = 110-120 °C (Table 4B). For every experiment, a high $M_{n,theo}$ was targeted (80-85 kg.mol^{-1}) to ensure a clear shift of the GPC peak. The final characterization of the chain-extended products is given in Table 4C.

Regarding *My*-rich macroinitiator *My*/GMA-78, a clean chain-extension with S was performed (experiment *My*/GMA-78-S) with a significant increase of M_n from 11.3 to 28.4 kg.mol^{-1} and Đ remaining low (< 1.40, Table 4C). The monomodal nature of P[(*My*-*stat*-GMA)-*b*-S] was confirmed by GPC as indicated in Figure 4a'. Furthermore, the GMA chain-extension from the same *My*/GMA-78 macroinitiator was attempted in order to deem the crossover efficiency. It has to be noted that around 10 mol% of *My* with respect to GMA was initially added (Table 4B). Indeed, NMP of GMA with 10 mol% of *My* (experiment *My*/GMA-10, Table 2) allowed to slow down the reaction with a pseudo-control of the polymerization (Đ ≤ 1.52 at X > 20 %, $M_n/M_{n,theo}$ > 80 % for every sample, Figure 2c) compared to the GMA homopolymerization by NMP ineffectively controlled by the SG1 free nitroxide. This observation echoes the comprehensive work done by Benoit *et al.*, reporting the well-controlled bulk NMP of *tert*-butyl acrylate and glycidyl methacrylate monomers at 120 °C in the presence of 10-20 mol% of isoprene and initiated by 2,2,5-trimethyl-3-(1′-phenylethoxy)-4-phenyl-3-azahexane[18]. This may suggest that the addition a small amount of isoprene or β-myrcene could improve the NMP control for certain methacrylate and acrylate monomers, presumably by reducing the average equilibrium constant of the system. Table 4C shows the final features of the chain-extended polymer (experiment *My*/GMA-78-GMA/*My*) and the GPC traces in the course

of the chain-extension are given in Figure 4a. Despite a slight broadening of the molecular weight distribution (Đ from 1.27 to 1.50), the chain-extension was successful with a monomodal shift of the GPC chromatograms and the addition of a GMA-rich second block exhibiting about 18 kg.mol^{-1}. While the macroinitiator was poor in GMA ($F_{GMA,1} = 0.22$), the chain-extension allowed to drastically alter the composition since the final diblock copolymer exhibited $F_{GMA,2} = 0.65$ (Table 4C), as determined by ^{1}H NMR.

In order to deem the influence of the composition of the *My*/GMA statistical copolymer over its ability to re-initiate cleanly a second batch of monomer, a GMA-rich P(*My*-*stat*-GMA) (*My*/GMA-37, $F_{GMA,1} = 0.63$, Table 4A) was used as a macroinitiator in the polymerization of *My* and S as described in Table 4B. For both experiments, a complete shift of the GPC peak (Figures 4b and 4b') corresponding to the addition of a P(*My*) segment exhibiting around 21 kg.mol^{-1} (experiment *My*/GMA-37-*My*) and the addition of a PS segment with $M_n \sim 27$ kg.mol^{-1} (experiment *My*/GMA-37-S, Table 4C) showed the effective synthesis of the diblock copolymer.

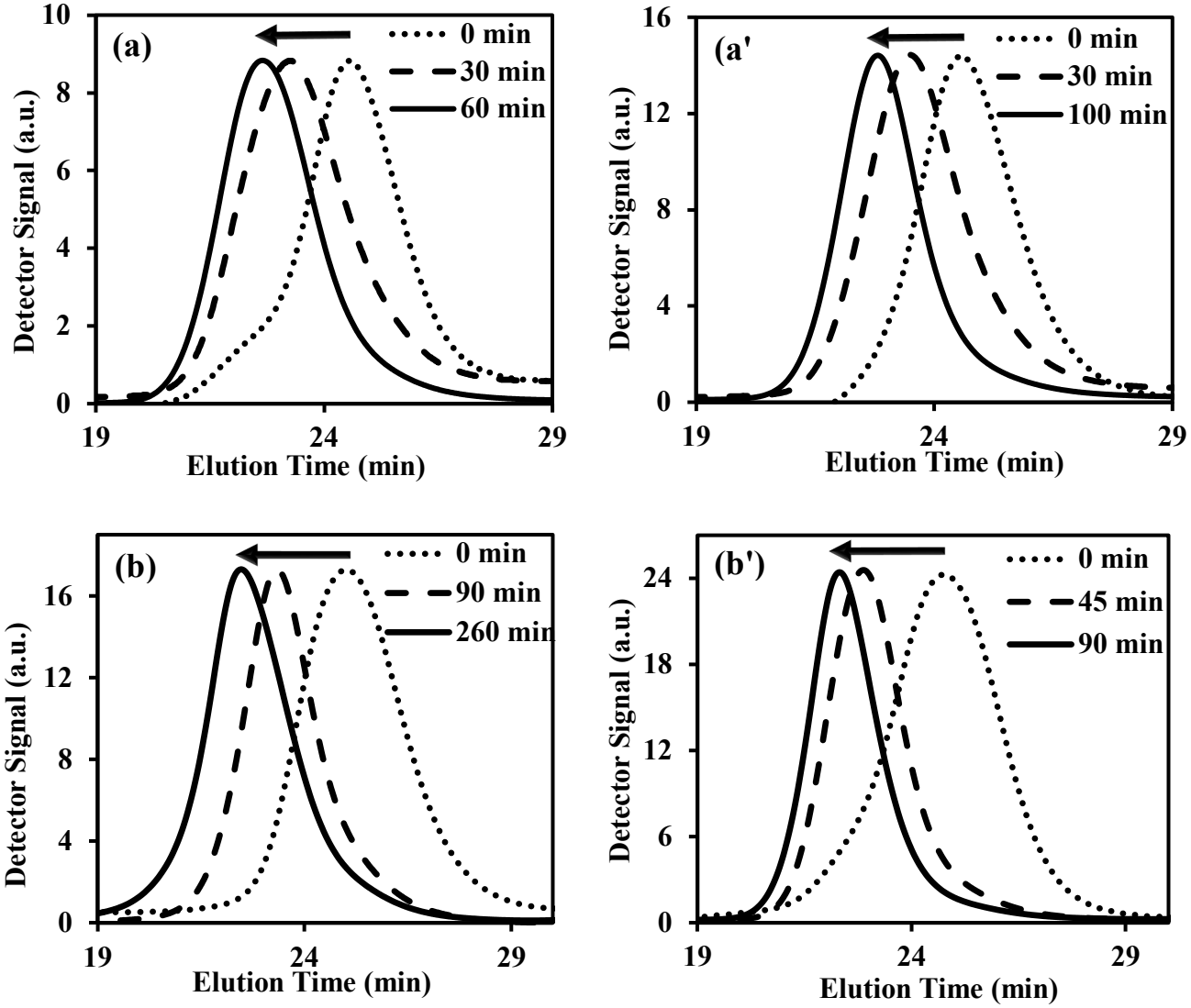

Figure 4. Normalized GPC traces for the chain-extensions of *My*/GMA-78 macroinitiator with **(a)** GMA with 10 mol% of *My* (experiment *My*/GMA-78-GMA/*My*) and **(a')** S (experiment *My*/GMA-78-S) and for the chain-extensions of *My*/GMA-37 macroinitiator with **(b)** *My* (experiment *My*/GMA-37-*My*) and **(b')** S (experiment *My*/GMA-37-S).

The ^{1}H NMR spectrum of final *My*/GMA-37-S diblock copolymer is given in Supporting Information, Figure S9, illustrating the ternary composition of the chain-extended product

synthesized. While a well-defined P[(*My-stat*-GMA)-*b*-S] was achieved ($Đ_2 = 1.46$, $M_{n,2}/M_{n,theo,X2} \sim 98$ %, Table 4C), *My* chain-extension from *My*/GMA-37 was not as well controlled, as seen by the broader molecular weight distribution ($Đ_2 = 1.85$) and the greater M_n deviation from the predicted one (~ 70 %). This marked loss of control may be explained by the more elevated temperature used ($T = 120$ °C to perform a faster *My* polymerization[39]) as well as the higher conversion reached ($X_2 = 45.3$ %). Another reason can also be mentioned. The polymerization was run for a relatively long period of time ($t = 260$ min) under a mild toluene reflux. A slight but gradual evaporation of the toluene was apparent during the experiment which, along with the consumption of *My*, made the reaction medium more and more viscous. A non-negligible influence of the viscosity, increasing with polymerization time, over the loss of control of the chain-extension can thereby be hypothesized. Moreover, the GPC samples at $t = 90$ min and 200 min (not included herein) exhibited $M_n = 19.8$ kg.mol^{-1}, $Đ = 1.40$ and $M_n = 25.9$ kg.mol^{-1}, $Đ = 1.51$ respectively, which demonstrates that the loss of control predominantly occurred during the last hour of the reaction. Generally, at the end of every chain-extension experiment, no major shoulder on the low molar mass side was detected, which indicates a low fraction of unreacted macroinitiator. However, a slight tail can be observed for long elution times (25-29 min) most likely resulting from irreversible terminations.

This study allowed to assess the presence of an alkoxyamine chain end for SG1 NMP-based P(*My-stat*-GMA) copolymers by ^{31}P NMR and chain-extensions. Regardless of their composition, P(*My-stat*-GMA) can thus be used as efficient macroinitiators in order to form versatile and well-defined diblock copolymers.

◘ Glass transition behavior of the synthesized *My*/GMA statistical and diblock copolymers.

Glass transition temperatures (T_g) were measured for the final P(*My*-*stat*-GMA) statistical copolymers exhibiting $F_{GMA} = 0.11$-0.95 (Table 3), by means of differential scanning calorimetry (see Experimental Section for further details, All the DSC traces are given in Supporting Information, Figure S10). T_g is depicted as a function of F_{GMA} in Figure 5. Each of the statistical copolymers showed a single T_g, which provided a concave glass transition temperature-composition curve. $T_{g,P(My)} = -77.0\ ^oC$[39] and $T_{g,P(GMA)} = +85.0\ ^oC$[80] corresponding to the T_g of P(My) and P(GMA) homopolymers have also been added in Figure 4 to serve as brackets for the copolymer T_gs. As expected, the concave trend reported indicates the non-ideal mixing of *My* and GMA, with the specific volume for P(*My*-*stat*-GMA) being larger than that for ideal mixing. This is likely due to the presence of the pendant flexible C6/C8 groups borne by the *My* units along the copolymer chain, which may alter the free volume. Several theoretical and empirical approaches have been proposed for estimating the T_g of mixtures and random copolymers from knowledge of the properties of the pure components[81-84]. Although different in detail, the proposed relationships are all based on the additivity of basic thermophysical properties. For the *My*/GMA system studied, they can be expressed by the Wood equation[84] as given below (Equation 5):

$$0 = W_{My}\,(T_g - T_{g,My}) + KW_{GMA}\,(T_g - T_{g,GMA}) \qquad \textbf{(5)}$$

where T_g corresponds to the theoretical glass transition temperature of the copolymer containing the weight fractions W_{My} and W_{GMA} of the two monomers. The Fox relationship[82] is obtained

when the parameter $K = T_{g,My} / T_{g,GMA}$. Interestingly, the Fox equation does not predict well the T_g versus composition relationship for the statistical *My*/GMA copolymers, as shown in Figure 5 (dotted line) by the overestimation of the copolymer T_gs (+ 19.4 °C on average) when using this simple bulk additive approach. Alternatively, the Gordon-Taylor equation[81] was used, relying still on Equation 5 but with $K = \Delta\beta_{GMA} / \Delta\beta_{My}$ where $\Delta\beta_{GMA}$ or $\Delta\beta_{My}$ is the difference between the expansion coefficients of the rubbery and glassy states of P(*GMA*) or P(*My*). $K = 0.186 \pm 0.036$ was estimated via the use of a non-linear least-squares fitting of the data and the Gordon-Taylor fit is given in Figure 5 (dashed line). $K \ll 1$ indicates that the volume expansion coefficient for GMA in the rubbery phase is significantly lower than that of *My*, according to the Gordon-Taylor approach. This appears very consistent since, above the glass transition temperature, it can be assumed that the expansivity of *My* is much greater than that of GMA, notably due its long pendant side group. On the other hand, stronger intermolecular forces are generated by GMA units, which might reduce its expansivity. To the best of our knowledge, the coefficients of thermal expansions (CTEs) for P(*My*) and P(GMA) are not available, limiting thus the discussion. However, it is useful to compare the results obtained via the Gordon-Taylor method for *My*/GMA to another system such as I/MMA. The CTE for the unvulcanized natural rubber (*cis*-1,4-poly(isoprene)) in the rubbery state (T = 0-20 °C) was estimated to be $6.6.10^{-4}$ K^{-1} [85] whereas the simulated value of its CTE in the glassy state was much lower, $2.0.10^{-4}$ K^{-1} at $T = -73$ °C[86]. Furthermore, the CTEs of atactic PMMA ($T_g \sim 105$ °C) in the rubbery state and in the glassy state are respectively $6.1.10^{-4}$ K^{-1} (T = 160 °C) and $1.8.10^{-4}$ K^{-1} (T = 40 °C)[85]. Consequently, $K = \Delta\beta_{MMA} / \Delta\beta_{I} = 0.93$ can be estimated for MMA/I system, indicating in that case a similar expansivity of both units in the rubbery phase.

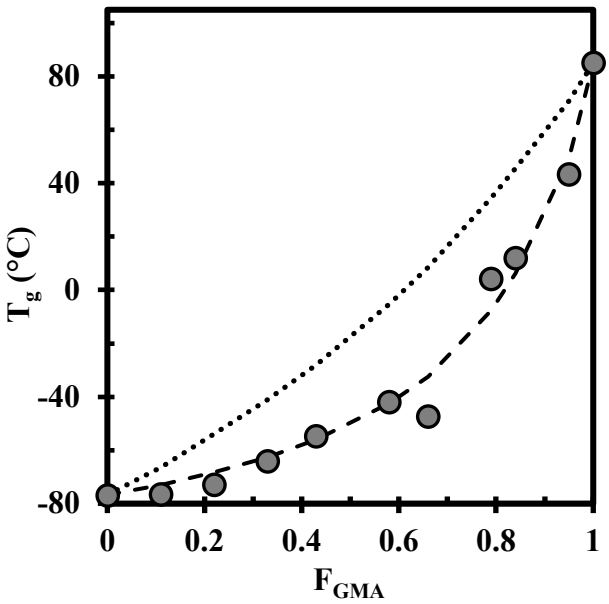

Figure 5. F_{GMA} effects on T_g in P(*My*-*stat*-GMA) statistical copolymers (grey circles). All of the DSC traces are given in the Supporting Information, Figure S10. The Fox equation[82] predictions of the P(*My*-*stat*-S) T_gs are represented by the dotted line while the dashed line represents the experimental data fitted to the Gordon-Taylor equation[81].

The T_g values of the diblock copolymers synthesized via chain-extensions were explored as well. The DSC traces for P(*My*-*stat*-GMA) macroinitiators and the resulting chain-extended products are given in Figure 6. While *My*-rich macroinitiator *My*/GMA-78 exhibited a single $T_g = -63.6$ °C relatively close to that of P(*My*) as predicted by Figure 5, two distinct T_gs were exhibited by the diblock copolymers *My*/GMA-78-GMA/*My* (-52.7 and $+15.8$ °C) and

My/GMA-78-S (− 27.1 and + 61.4 ºC). Such a thermal behavior is typical of the presence of two heterogeneous phases, highlighting herein the high degree of chemical incompatibility between *My*/GMA-78 block and the chain-extended block. Interestingly, the lower T_g of these diblock copolymers (− 52.7 and − 27.1 ºC) does not correspond exactly to that of the parent macroinitiator (− 63.6 ºC). This is particularly marked with *My*/GMA-78-S having a subzero T_g significantly higher than that of *My*/GMA-78, which may reflect the partial mixing of the two block phases. Likewise, the above-zero T_gs of *My*/GMA-78-GMA/*My* (+ 15.8 ºC) and *My*/GMA-78-S (+ 61.4 ºC) are lower than *My*/GMA-10 T_g (+ 43.2 ºC) and PS T_g (~ 96 ºC for M_n ~ 17 kg.mol^{-1} [87]) respectively, supporting the possible partial miscibility between the soft and the hard blocks.

On the contrary, the two T_gs of the diblock *My*/GMA-37-*My* (− 78.1 ºC and − 7.3 ºC, Figure 6a) corresponded almost to those of the P(*My*) homopolymer (− 77 ºC[39]) and the initial *My*/GMA-37 macroinitiator (− 12.0 ºC, Figure 6a). Accordingly, a stronger incompatibility between the two blocks may be apparent, bringing about a much more distinct two-phase microstructure. This could result from the long hydrocarbon pendant groups of *My* units, increasing significantly the free volume and the steric hindrance around P(*My*) chains and thus reinforcing the heterogeneity of the two-phase system. Regarding *My*/GMA-37-S, only the upper T_g was observed at + 67.5 ºC (Figure 6a). The disappearance of the parent macroinitiator T_g can be due to the large difference in M_n between the two blocks (8.6 and 26.8 kg.mol^{-1} for *My*/GMA-37 and PS respectively, Table 4) combined with the relatively short average chain length of *My*/GMA-37.

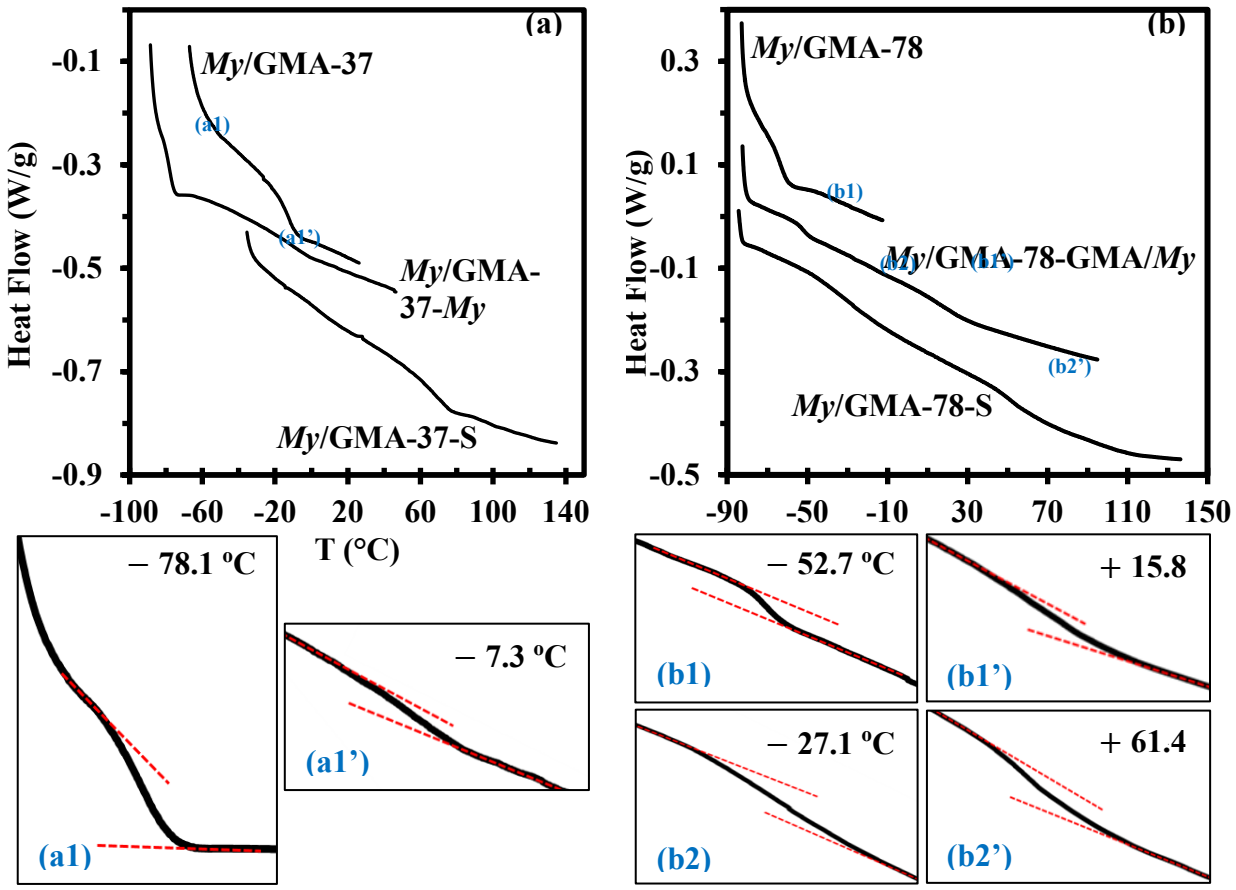

Figure 6. DSC traces (second heating run) of **(a)** *My*/GMA-37 macroinitiator, *My*/GMA-37-*My* and My/GMA-37-S diblock copolymers and **(b)** *My*/GMA-78 macroinitiator, *My*/GMA-78-GMA/*My* and *My*/GMA-78-S diblock copolymers. The dashed blue lines indicate the changes in slope observed. Magnifications with T_g values are given below the plotsfor the changes in slope harder to observe, as indicated by the blue indexes in brackets,.

Generally, these DSC measurements suggest the possible microphase separation of the synthesized diblocks. In such instance, the use of a homopolymer as macroinitiator instead of a statistical copolymer and blocks exhibiting a higher degree of polymerization should favor a neater separation of the phases. The Flory-Huggins interaction parameter χ[88] measuring the differences in the strength of pairwise interaction energies between species can be estimated for the *My*/GMA system using Equation 6 (Hildebrand and Scott method)[89]:

$$\chi_{My\text{-GMA}} = V_{m,GMA} (\delta_{My} - \delta_{GMA})^2 / RT \qquad \textbf{(6)}$$

where $V_{m,GMA}$ is the molar volume of GMA (136.4 $cm^3.mol^{-1}$) considered as the ``solvent``(lower molecular weight), δ_{My} and δ_{GMA} are the solubility parameters of *My* and GMA respectively and R corresponds to the ideal gas constant (8.314 $J.mol^{-1}.K^{-1}$). $\delta_{My} = 16.2$ $MPa^{1/2}$ and $\delta_{GMA} = 19.3$ $MPa^{1/2}$ were calculated, using the reported Hansen solubility parameters for *My*[90] and GMA[91], which gives $\chi_{My\text{-GMA}} = 0.50$ at T = 25 ºC (see Supporting Information, page S13, for the calculations). In order to estimate the miscibility between the P(*My*) and P(GMA) blocks, a mixture of 1 g of P(My) and 1 g of P(GMA) with $M_{n,P(My)} = M_{n,P(GMA)} = 15$ $kg.mol^{-1}$ can be arbitrarily considered as an example. The Gibbs free energy ΔG_m for this binary P(*My*)/P(GMA) polymer mixture can be estimated using the equation developed by Flory and Huggins[92] as given in Equation 7:

$$\Delta G_M = kT [(V/V_r) \upsilon_{P(GMA)} \upsilon_{P(My)} \chi_{My\text{-GMA}} (1 - 2/z) + N_c (\upsilon_{P(GMA)} ln(\upsilon_{P(GMA)}) + \upsilon_{P(My)} ln(\upsilon_{P(My)})] \qquad \textbf{(7)}$$

where *k* is the Boltzmann's constant, *V* is the total volume of the mixture, V_r is the molar of a specific segment, v_i is the volume fraction of polymer ''*I*'', *z* is the lattice coordination number (usually between 6 and 12) and N_c is the number of chains per volume unit. ΔG_M (25 ºC, z = 6) = 2.52 J was calculated when assuming that the number of lattice sites per chain is 6 (usually chosen for estimating polymer mixture miscibility[93]). Consequently, ΔG_M (25 ºC, z = 6) > 0 indicates that P(*My*)/P(GMA) system with $M_{n,P(My)} = M_{n,P(GMA)} = 15$ $kg.mol^{-1}$ is not miscible at T = 25 ºC, according to the Flory-Huggins theory. The upper limiting $M_{n,lim}$ number-average molecular weight value allowing the P(*My*)/P(GMA) system to be miscible at T = 25 ºC can be calculated for ΔG_M (25 ºC, z = 6) = 0 as well. $M_{n,lim} \sim 1.2$ $kg.mol^{-1}$ was estimated, indicating

that a homogeneous mixture of 1 g of P(*My*) and 1 g of P(GMA) with $M_{n,P(My)} = M_{n,P(GMA)} \leq 1.2$ kg.mol^{-1} could be achieved at room temperature (see Supporting Information, page S14, for the calculations). Even though this Flory-Huggins thermodynamic model does not account for a change of volume upon mixing to name but one limitation, it supports theoretically the possible phase separation of *My*/GMA diblock copolymer. Obviously, direct experimental characterization using techniques such as transmission electron microscopy (TEM) or small-angle X-ray scattering (SAXS) should be done to unequivocally demonstrate whether a microphase separation is apparent. Regardless, in the context of the present study, the nature of the polymerization process (using statistical copolymer segments) influenced the thermal properties, not surprisingly showing some diffuse interfacial effects on the miscibility of the block copolymer segments.

C) Synthesis of poly(β-myrcene-*block*-2-hydroxy-3-morpholinopropyl methacrylate) P(*My*-*b*-HMPMA) amphiphilic diblock copolymer by SG1-based NMP.

The well-controlled nitroxide-mediated copolymerization of *My* and GMA in bulk initiated by NHS-BB allowed the synthesis of epoxide functionalized *My*-based polymers. Once the polymer is produced, different chemical transformations of the epoxy groups can be performed to obtain a series of polymers with varied properties. In this study, we tried to synthesize an amphiphilic diblock copolymer in a three-step process: (1) NMP of *My*; (2) GMA chain-extension

from NMP-based P(*My*) macroinitiator; (3) Post-polymerization treatment using morpholine to yield poly(β-myrcene-*block*-2-hydroxy-3-morpholinopropyl methacrylate) P(*My*-*b*-HMPMA) diblock copolymer. The synthesis route is shown in Figure 7.

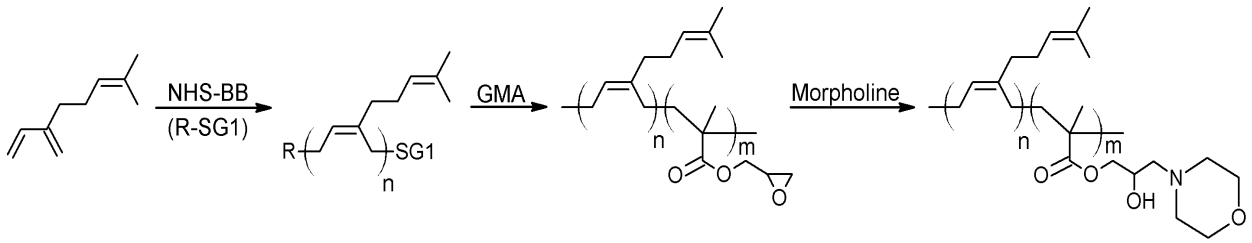

Figure 7. Synthetic route for P(*My*-*b*-HMPMA) diblock copolymer.

Firstly, NHS-BB-mediated P(*My*) exhibiting M_n = 14.4 kg.mol^{-1} and Đ = 1.51 was synthesized in bulk at 120 °C after 6 h of polymerization. The chain-extension of this NMP-based polyterpene with 90 mol% of GMA and 10 mol% of *My* was then performed for 50 min at 110 °C in 50 wt% of toluene. The resulting P(*My*-*b*-GMA) diblock copolymer had M_n = 23.8 kg.mol^{-1}, Đ = 1.89 and F_{My} = 0.58 (^{1}H NMR spectrum in Figure 8a) and the epoxy groups, inert towards the previous polymerization process, were lastly treated with a 6-fold amount of morpholine in refluxing Me-THF for 3 h at 77 °C (complete experimental conditions and results for each step summed up in Supporting Information, Table S2), relying on the comprehensive study led by Benaglia and coworkers[94]. This ring-opening reaction of the pendant epoxides proceeded quantitatively as shown by the ^{1}H NMR spectrum of the resulting P(*My*-*b*-HMPMA) diblock copolymer in Figure 8.

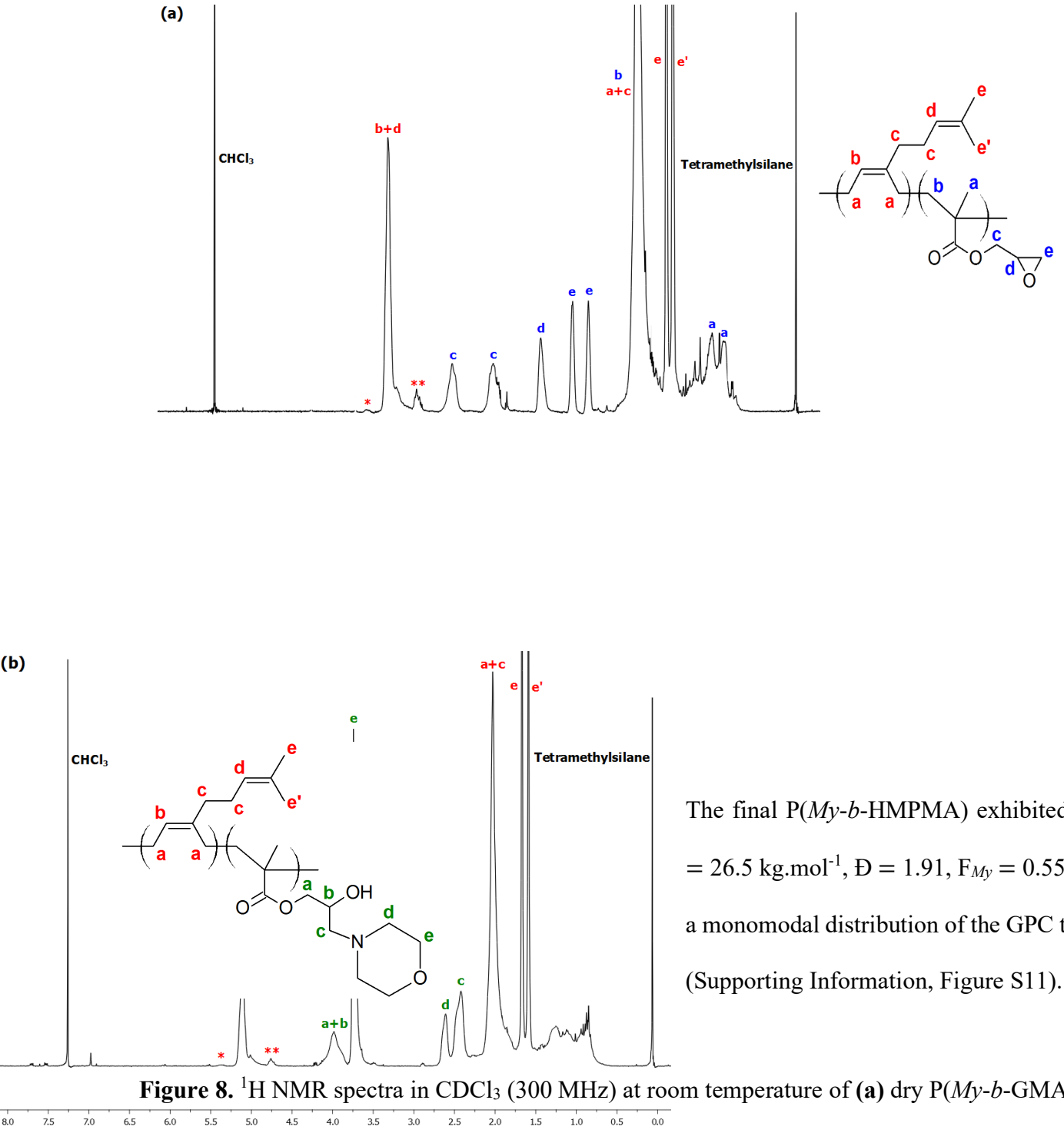

Figure 8. ^{1}H NMR spectra in $CDCl_3$ (300 MHz) at room temperature of **(a)** dry P(*My*-*b*-GMA) diblock copolymer and **(b)** the resulting dry P(*My*-*b*-HMPMA) after treatment with morpholine. Tetramethylsilane was used as an internal reference. The assignments * and ** refer to olefinic and vinyl protons of 1,2- and 3,4-P(*My*) contents.

The final P(*My*-*b*-HMPMA) exhibited M_n = 26.5 kg.mol^{-1}, Đ = 1.91, F_{My} = 0.55 and a monomodal distribution of the GPC trace (Supporting Information, Figure S11). The

slight increase of M_n after the treatment with morpholine may be explained by the occurrence of branching reactions, as reported previously[94].

The behavior of this morpholine derivatized P(*My*-*b*-HMPMA) in water was then explored by dynamic light scattering (DLS) to determine if this diblock copolymer is able to self-assemble under specific conditions. The polymer was first dissolved in a minimum amount of THF, which is a good solvent for both P(*My*) and P(GMA) segments, and then added in a water (purified by reverse osmosis) solution, followed by intense dispersion. The suspension was heated at 50 °C for 30 min and the THF was then eliminated by dialysis. A homogeneous clear aqueous solution was obtained. Regarding the samples used, two parameters were changed, [P(*My*-*b*-HMPMA)] = 0.4-1.4 mg.ml^{-1} and the duration of the stirring (three days to ten days), as indicated in Table 5. Furthermore, the DLS measurements were carried out for every sample at three different temperatures, T_{DLS} = 25, 45 and 65 °C. It should be first noted that a monomodal distribution was observed for every sample, with a DLS polydispersity index relatively high for experiments conducted at room temperature (PDI = 0.24 on average at T = 25 °C) and more satisfactory at T = 45-65 °C (PDI = 0.10 on average). The relatively low PDI values make the Z-average size reliable and was reported in this study. Regardless of preparation of the samples, as T_{DLS} increased from 25 to 45 °C, a marked drop of the Z-average diameter (Z_{ave}) was noticeable (105 nm drop on average). However, increasing T_{DLS} from 45 to 65 °C did not result in a further Z_{ave} decrease. The set of experiments III (Table 5) can be taken as an example. While large aggregates were detected at room temperature (> 300 nm), a second population of aggregates exhibiting a smaller hydrodynamic diameter (~ 130 nm) was obtained at 45 °C and 65 °C. Accordingly, a critical temperature (T_{cri}) between 25 and 45 °C might favour the formation of micelles exhibiting a lower hydrodynamic diameter. It was well-reported that the behavior of a polymeric micellar system

toward temperature mostly depend on the nature of the hydrophilic block[95,96]. For P(My-b-HMPMA) diblock copolymer, the decrease of Z_{ave} at T ≥ 45 °C may be explained by the much lower solvation of the P(GMA) segments in the corona of the micelles. Four different preparations were performed before measuring the DLS samples, from a relatively high concentration (1.4 mg.ml^{-1}) with a short period of stirring (3 days, I, Table 5) to a low concentration (0.4 mg.ml^{-1}) combined with a long period of stirring (10 days, IV, Table 5). The influence of the concentration over Z_{ave} can be assessed by comparing the DLS results between the first (I) and the second (II) preparation, where samples were stirred for 3 days. Regardless of T_{DLS}, a clear decrease of Z_{ave} was effective when reducing [P(*My*-*b*-HMPMA)] from 1.4 to 1.0 mg.ml^{-1}. Generally, as the time of stirring increased and the concentration of the copolymer decreased, a clear reduction of Z_{ave} was observed. The aggregations of the micelles may be limited by reducing [P(*My*-*b*-HMPMA)] and/or stirring rigorously for 6 days or more. It can be assumed that stirring allowed to homogenously disperse the particles in the water solution whereas a lower [P(*My*-*b*-HMPMA)] diminished statistically the formation of large aggregates.

Even though other experimental conditions could be used to characterize the self-assembly of P(*My*-*b*-HMPMA) exhibiting M_n = 26.5 kg.mol^{-1} and F_{My} = 0.55, the study led herein suggests that micelles having Z_{ave} = 120-130 nm can be formed in water at T = 45-65 °C and [P(*My*-*b*-HMPMA)] ≤ 0.7 mg.ml^{-1}, after a few days of stirring.

Table 5. Dynamic light scattering analyses of 1.4, 1.0, 0.7 and 0.4 mg.ml^{-1} od P(*My*-*b*-HMPMA) in reversed osmosis water solution performed at 25, 45 and 65 °C.

Preparation[c]	Z_{ave}[a] (nm) / PDI[b]			
	I. 1.4 mg.ml^{-1} Stir for 3 days	**II.** 1.0 mg.ml^{-1} Stir for 3 days	**III.** 0.7 mg.ml^{-1} Stir for 6 days	**IV.** 0.4 mg.ml^{-1} Stir for 10 days
T_{DLS}[d] = 25 ºC	341 ± 19 / 0.24	268 ± 21 / 0.16	309 ± 15 / 0.29	214 ± 15 / 0.27
T_{DLS} = 45 ºC	266 ± 8 / 0.07	198 ± 6 / 0.10	129 ± 17 / 0.11	119 ± 12 / 0.13
T_{DLS} = 65 ºC	275 ± 9 / 0.09	168 ± 12 / 0.09	134 ± 9 / 0.12	120 ± 16 / 0.11

a) Z-average diameter (cumulants mean) derived from three separate repeats. The error is given as the standard deviation from the three separate repeats.

b) Polydispersity Index (PDI) corresponds to the coefficient of the squared term ‘’c’’ when scaled as $2c/b^2$, where ‘’b’’ and ‘’c’’ are obtained from the cumulants analysis, which fits a polynomial to the log of the G_1 correlation function.

c) [P(My-b-HMPMA)] = 0.4-1.4 mg.ml^{-1} in reversed osmosis water was studied

d) T_{DLS} corresponds to the temperature set during the DLS analysis.

CONCLUSION.

The possibility of synthesizing well-tailored *My*/methacrylate copolymers by NMP has been supported by the satisfactory stoichiometric copolymerization of *My* and MMA in bulk at 110 °C initiated by NHS-BB. The linear relationship between M_n and X combined with Đ as low as 1.15-1.32 shown by this polymerization prompted us to study the NMP of *My* with GMA, a highly versatile monomer bearing an epoxy group. *My*/GMA NMP with $f_{My,0} = 0.10\text{-}0.90$ was performed in bulk at 120 °C initiated by NHS-BB. $r_{My} = 0.80 \pm 0.31$ and $r_{GMA} = 0.71 \pm 0.15$ were determined by the FR approach whereas the KT method gave $r_{My} = 0.48 \pm 0.12$ and $r_{GMA} = 0.53 \pm 0.18$. The statistical nature of this copolymerization was confirmed using a NLLS procedure yielding $r_{My} = 0.49 \pm 0.13$ and $r_{GMA} = 0.50 \pm 0.13$. For $f_{My,0} = 0.60\text{-}0.90$, well-defined P(*My*-*stat*-GMA) copolymers were achieved with M_n approximately 81 % of $M_{n,theo}$ and Đ = 1.26-1.35 at X as high as 79-89 %. Even though broader molecular weight distributions (Đ = 1.35-1.55) were measured for GMA-rich initial feeds ($f_{My,0} = 0.10\text{-}0.49$) during the copolymerizations, the linear increase of M_n with X and the monomodal nature of the GPC peaks indicated the satisfactory mediation of these reactions by SG1. The more apparent loss of control observed for *My*/GMA copolymerizations exhibiting richer GMA initial concentrations was likely due to the significantly higher propagation rate as indicated by $\langle k_p \rangle \langle K \rangle = (157.0 \pm 0.9)\ 10^{-5}\ s^{-1}$ at $f_{GMA,0} = 0.90$, about 36 times higher than that of *My* NMP under the same reaction conditions ($\langle k_p \rangle \langle K \rangle = (4.3 \pm 0.7)\ 10^{-5}\ s^{-1}$). The faster kinetics presumably favored the occurrence of irreversible terminations which might be β-hydrogen transfer from propagating P(*My*-*stat*-GMA) radical to SG1 or intramolecular chain transfer to polymer. P(*My*-*stat*-GMA)s exhibiting $F_{GMA} = 0.11\text{-}0.95$ displayed a range of T_gs from – 77 °C to + 43 °C. *My*-rich and GMA-rich P(*My*-*stat*-GMA)s were cleanly chain-extended with *My*, S and GMA, indicating the

high chain-end fidelity of these macroinitiators, which was also confirmed by the quantitative estimation of the SG1 end-group via ^{31}P NMR (LF = 82 ± 5 % and 71 ± 7 % respectively). Most of the resulting diblock copolymers exhibited two distinct T_gs, indicative of a possible microphase separation. Lastly, a NMP-based P(*My*-*b*-GMA) diblock copolymer was treated with morpholine, a nucleophilic reagent, to yield quantitatively P(*My*-*b*-HMPMA). This latter exhibited a higher degree of hydrophilicity, as shown by its total dissolution in water, compared to P(*My*-*b*-GMA). P(*My*-*b*-HMPMA) was able to self-organize into micelles in water, exhibiting Z_{ave} = 120-130 nm at T = 45-65 °C and [P(*My*-*b*-HMPMA)] ≤ 0.7 mg.ml^{-1}. Thus, well-tailored statistical and diblock epoxide functionalized P(*My*)s can be readily synthesized by SG1-mediated NMP, opening the door to a multitude of post-polymerization treatments resulting in the achievement of multifunctional *My*-based polymers.

ASSOCIATED CONTENT

Supporting Information

The Supporting Information is available free of charge on the ACS Publications website.

Detailed kinetics of *My*/YY copolymerizations (YY = MA, MMA, *t*BuA), theoretical background (FR, KT and NLLS approaches) and experimental details for *My*/GMA statistical copolymerization, ^{1}H and ^{31}P NMR spectra and additional DSC traces for statistical P(*My*-*stat*-GMA) copolymers, Theoretical estimation of ΔG_m, GPC traces and DLS curves for P(*My*-*b*-HMPMA) diblock copolymer.

AUTHOR INFORMATION

Corresponding Author

*E-mail: milan.maric@mcgill.ca (M.M.)

ACKNOWLEDGMENTS

ArianeGroup and the French Defense Procurement Agency (DGA) supported this work financially. We thank the Center for Self Assembled Chemical Structures (CSACS, McGill University) for the use of the DSC and the TGA. We also thank Mary Sullivan and Noah Macy of Arkema for their aid in obtaining the BlocBuilder™ alkoxyamine initiator.

REFERENCES

(1) Shanks, R. A.; Kong, I. General Purpose Elastomers: Structure, Chemistry, Physics and Performance. In *Advances in Elastomers I: Blends and Interpenetrating Networks*; Visakh, P. M., Thomas, S., Chandra, A. K., Mathew, A. P., Eds.; Springer-Verlag: Berlin, **2013**; 11-45.

(2) Ridha, R. A.; Curtiss, W. W. Developments in Tire Technology. In *Rubber Products Manufacturing Technology*; Bhowmick, A. K., Hall, M. M., Benarey, H. A., Eds.; Marcel Dekker, Inc.: New York, **1994**; 533-564.

(3) Akelah, A.; Moet, A. *Functionalized Polymers and Their Applications*; Chapman and Hall: New York, 1990.

(4) Li, L.; Li, S.; Cui, D. Highly *Cis*-1,4-Selective Living Polymerization of 3-Methylenehepta-1,6-diene and its subsequent Thiol-Ene Reaction: An Efficient Approach to Functionalized Diene-based Elastomer. *Macromolecules* **2016**, *49*, 1242-1251.

(5) Abd Rabo Moustafa, M. M.; Gillies, E. R. Rubber Functionalization by Diels-Alder Chemistry: From Cross-Linking to Multifonctional Graft Copolymer Synthesis. *Macromolecules* **2013**, *46*, 6024-6030.

(6) Grubbs, R. B.; Broz, M. E.; Dean, J. M.; Bates, F. S. Selectively Epoxidized Polyisoprene-Polybutadiene Block Copolymers. *Macromolecules* **2000**, *33*, 2308-2310.

(7) Wongthong, P.; Nakason, C.; Pan, Q.; Rempel, G. L.; Kiatkamjornwong, S. Modification of Deproteinized Natural Rubber via Grafting Polymerization with Maleic Anhydride. *Eur. Polym. J.* **2013**, *49*, 4035-4046.

(8) Teyssié, P.; Julemont, M.; Thomassin, J. M.; Walckiers, E.; Warin, R. Stereospecific Coordination of Diolefins by h^3-Allylic Coordination Complexes. In *Coordination Polymerization: A Memorial to Karl Ziegler*; Chien, J. C. W., Ed.; Academic Press, Inc.: New York, **1975**; 327-348.

(9) Zhang, Z.; Cui, D.; Wang, B.; Liu, B.; Yang, Y. Polymerization of 1,3-Conjugated Dienes with Rare-Earth Metal Precursors. In *Molecular Catalysis of Rare-Earth Elements*; Roesky, P. W., Ed.; Springer: Berlin, **2010**; 49-108.

(10) Nishikawa, M.; Maeda, M.; Nakata, H.; Takamatsu, H.; Ishii, M. New Isoprene Polymers. In *Applications of Anionic Polymerization Research*; Quirk, R. P., Ed.; Oxford University Press: Washington, 1998; 186-196.

(11) Arest-Yakubovich, A. A.; Goldberg, I. P.; Zolotarev, V. L.; Aksenov, V. I.; Ermakova, I. I.; Ryakhovsky, V. S. Commercial Production of 1,2-Polybutadiene. In *Applications of Anionic*

Polymerization Research; Quirk, R. P., Ed.; Oxford University Press: Washington, 1998; 197-206.

(12) Nozaki, K. Polymerization of Polar Monomers. In *Organometallic Reactions and Polymerization*; Osakada, K., Ed.; Springer: Berlin, **2014**; 217-236.

(13) Chiefari, J.; Chong, Y.; Ercole, F.; Krstina, J.; Jeffery, J.; Le, T.; Mayadunne, R.; Meijs, G.; Moad, C.; Moad, G.; Rizzardo, E.; Thang, S. Living Free-Radical Polymerization by Reversible Addition-Fragmentation Chain Transfer: The RAFT Process. *Macromolecules* **1998**, *31*, 5559−5562.

(14) Braunecker, W. A.; Matyjaszewski, K. Controlled/Living Radical Polymerization: Features, Developments, and Perspectives. *Prog. Polym. Sci.* **2007**, *32* (1), 93−146.

(15) Georges, M. K.; Veregin, R. P. N.; Kazmaier, P. M.; Hamer, G. K. Narrow Molecular Weight Resins by a Free-Radical Polymerization Process. *Macromolecules* **1993**, *26* (11), 2987−2988.

(16) Veregin, R. P. N.; Georges, M. K.; Kazmaier, P. M.; Hamer, G. K. Free Radical Polymerizations for Narrow Polydispersity Resins: Electron Spin Resonance Studies of the Kinetics and Mechanism. *Macromolecules* **1993**, *26* (20), 5316−5320.

(17) Wang, J.-S.; Matyjaszewski, K. Controlled/"Living" Radical Polymerization. Atom Transfer Radical Polymerization in the Presence of Transition-Metal Complexes. *J. Am. Chem. Soc.* **1995**, *117* (20), 5614−5615.

(18) Benoit, D.; Harth, E.; Fox, P.; Waymouth, R. M.; Hawker, C. J. Accurate Structural Control and Block Formation in the Living Polymerization of 1,3-Dienes by Nitroxide-Mediated Procedures. *Macromolecules* **2000**, *33*, 363-370.

(19) Hua, J.; Li, X.; Li, Y. -S.; Xu, L.; Li, Y. –X. Atom Transfer Radical Polymerization of Butadiene using MoO_2Cl_2/PPh3 as the catalyst. *J. Appl. Polym. Sci.* **2007**, *104* (6), 3517-3522.

(20) Wei, R.; Luo, Y.; Li, Z. Synthesis of Structured Nanoparticles of Styrene/Butadiene Block Copolymers via RAFT seeded Emulsion Polymerization. *Polymer* **2010**, *51* (17), 3879-3886.

(21) Hlalele, L.; D`Hooge, D. R.; Dürr, C. J.; Kaiser, A.; Brandau, S.; Barner-Kowollik, C. RAFT-Mediated *ab Initio* Emulsion Copolymerization of 1,3-Butadiene with Acrylonitrile. *Macromolecules* **2014**, *47* (9), 2820-2829.

(22) Zhu, J.; Zhou, D.; Zhu, X.; Chen, G. Reversible Addition-Fragmentation Chain Transfer Polymerization of Glycidyl Methacrylate with 2-Cyanoprop-2-yl 1-Dithionaphthalate as a Chain-transfer Agent. *J. Polym. Sci., Part A: Polym. Chem.* **2004**, *42* (10), 2558-2565.

(23) Solomon, D. H.; Rizzardo, E.; Cacioli, P. New Polymerization Process and Polymers Produced Thereby. *Eur. Pat. Appl.* 0135280A3, **1985**.

(24) Fukuda, T.; Terauchi, T.; Goto, A.; Ohno, K.; Tsujii, Y.; Miyamoto, T.; Kobatake, S.; Yamada, B. Mechanisms and Kinetics of Nitroxide-Controlled Free Radical Polymerization. *Macromolecules* **1996**, *29* (20), 6393-6398.

(25) Nicolas, J.; Guillaneuf, C.; Lefay, C.; Bertin, D.; Gigmes, D.; Charleux, B. Nitroxide-Mediated Polymerization. *Prog. Polym. Sci.* **2013**, *38* (1), 63-235.

(26) Grubbs, R. B. Nitroxide-Mediated Radical Polymerization: Limitations and Versatility. *Polym. Rev.* **2011**, *51* (2), 104-137.

(27) Hawker, C. J. ``Living`` Free Radical Polymerization: A Unique Technique for the Preparation of Controlled Macromolecular Architectures. *Acc. Chem. Res.* **1997**, *30* (9), 373-382.

(28) Benoit, D.; Chaplinski, V.; Braslau, R.; Hawker, C.J. Development of a Universal Alkoxyamine for ``Living`` Free Radical Polymerizations. *J. Am. Chem. Soc.* **1999**, *121*, 3904-3920.

(29) Benoit, D.; Grimaldi, S.; Robin, S.; Finet, J. –P.; Tordo, P.; Gnanou, Y. Kinetics and Mechanism of Controlled Free-Radical Polymerization of Styrene and *n*-Butyl Acrylate in the Presence of an Acyclic β-Phosphonylated Nitroxide. *J. Am. Chem. Soc.* **2000**, *122* (25), 5929-5939.

(30) Rodlert, M.; Harth, E.; Rees, I.; Hawker, C. J. End-group Fidelity in Nitroxide-Mediated Living Free-radical Polymerizations. *J. Polym. Sci., Part A: Polym. Chem.* **2000**, *38*, 4749-4763.

(31) Cheng, C.; Qi, K.; Khoshdel, E.; Wooley, K. L. Tandem Synthesis of Core-shell Brush Copolymers and their Transformation to Peripherally Cross-linked and Hollowed Nanostructures. *J. Am. Chem. Soc.* **2006**, *128* (21), 6808-6809.

(32) Hill, N. L.; Braslau, R. Synthesis and Characterization of a Novel Bisnitroxide Initiator for Effecting ``Outside-In`` Polymerization. *Macromolecules* **2005**, *38* (22), 9066-9074.

(33) Ruehl, J.; Nilsen, A.; Born, S.; Thoniyot, P.; Xu, L. P.; Chen, S.; Braslau, R. Nitroxide-Mediated Polymerization to Form Symmetrical ABA Triblock Copolymers from a Bidirectional Alkoxyamine Initiator. *Polymer* **2007**, *48* (9), 2564-2571.

(34) Lohmeijer, B. G. G.; Schubert, U. S. The LEGO Toolbox: Supramolecular Building Blocks by Nitroxide-Mediated Controlled Radical Polymerization. *J. Polym. Sci., Part A: Polym. Chem.* **2005**, *43*, 6331-6344.

(35) Wegrzyn, J. K.; Stephan, T.; Lau, R.; Grubbs, R. B. Preparation of Poly(ethylene oxide)-*block*-Poly(isoprene) by Nitroxide Mediated Free Radical Polymerization from PEO Macroinitiators. *J. Polym. Sci., Part A: Polym. Chem.* **2005**, *43* (14), 2977-2984.

(36) Sundararaman, A.; Stephan, T.; Grubbs, R. B. Reversible Restructuring of Aqueous Block Copolymer Assemblies through Stimulus-Induced Changes in Amphiphilicity. *J. Am. Chem. Soc.* **2008**, *130* (37), 12264-12265.

(37) Cai, Y.; Aubrecht, K. B.; Grubbs, R. B. Thermally Induced Changes in Amphiphilicity Drive Reversible Restructuring of Assemblies of ABC Triblock Copolymers with Statistical Polyether Blocks. *J. Am. Chem. Soc.* **2011**, *133* (4), 1058-1065.

(38) Harrisson, S.; Couvreur, P.; Nicolas, J. SG1 Nitroxide-Mediated Polymerization of Isoprene: Alkoxyamine Structure/Control Relationship and α,ω-Chain-End Functionalization. *Macromolecules* **2011**, *44* (23), 9230−9238.

(39) Métafiot, A.; Kanawati, Y.; Gérard, J. –F.; Defoort, B.; Maric, M. Synthesis of β-Myrcene-Based Polymers and Styrene Block and Statistical Copolymers by SG1 Nitroxide-Mediated Controlled Free Radical Polymerization. *Macromolecules* **2017**, *50* (8), 3101-3120.

(40) Moayeri, A.; Lessard, B.; Marić, M. Nitroxide Mediated Controlled Synthesis of Glycidyl Methacrylate-Rich Copolymers enabled by SG1-based Alkoxyamines bearing Succinimidyl Ester Groups. *Polym. Chem.* **2011**, *2*, 2084−2092.

(41) Zhang, C.; Marić, M. Synthesis of Stimuli-Responsive, Water-Soluble Poly[2-(dimethylamino)ethyl methacrylate/styrene] Statistical Copolymers by Nitroxide Mediated Polymerization. *Polymers* **2011**, *3* (3), 1398−1422.

(42) Marić, M.; Consolante, V. Versatility of a Succinimidyl-Ester Functional Alkoxyamine for Controlling Acrylonitrile Copolymerizations. *J. Appl. Polym. Sci.* **2013**, *127*, 3645−3656.

(43) Vinas, J.; Chagneux, N.; Gigmes, D.; Trimaille, T.; Favier, A.; Bertin, D. SG1-based Alkoxyamine bearing a *N*-Succinimidyl Ester: A Versatile Tool for Advanced Polymer Synthesis. *Polymer* **2008**, *49* (17), 3639−3647.

(44) Farcet, C.; Belleney, J.; Charleux, B.; Pirri, R. Structural Characterization of Nitroxide-Terminated Poly(*n*-butyl acrylate) Prepared in Bulk and Miniemulsion Polymerizations. *Macromolecules* **2002**, *35* (13), 4912-4918.

(45) Farcet, C.; Charleux, B.; Pirri, R. Poly(*n*-butyl acrylate) Homopolymer and Poly[*n*-butyl acrylate-*b*-(*n*-butyl acrylate-*co*-styrene)] Block Copolymer Prepared via Nitroxide-Mediated Living/Controlled Radical Polymerization in Miniemulsion. *Macromolecules* **2001**, *34* (12), 3823-3826.

(46) Nicolas, J.; Dire, C.; Mueller, L.; Belleney, J.; Charleux, B.; Marque, S. R. A.; Bertin, D.; Magnet, S.; Couvreur, L. Living Character of Polymer Chains prepared via Nitroxide-Mediated

Controlled Free-Radical Polymerization of Methyl Methacrylate in the Presence of a Small Amount of Styrene at Low Temperature. *Macromolecules* **2006**, *39* (24), 8274-8282.

(47) Nicolas, J.; Brusseau, S.; Charleux, B. A Minimal Amount of Acrylonitrile Turns the Nitroxide-Mediated Polymerization of Methyl Methacrylate iasuanto an almost Ideal Controlled/Living System. *J. Polym. Sci., Part A: Polym. Chem.* **2010**, *48* (1), 34-47.

(48) Trumbo, D. L. Free Radical Copolymerization Behavior of Myrcene: I. Copolymers with Styrene, Methyl Methacrylate or p-Fluorostyrene. *Polym. Bull.* **1993**, *31*, 629−636.

(49) Sarkar, P.; Bhowmick, A. K. Synthesis, Characterization and Properties of a Bio-based Elastomer: Polymyrcene. *RSC Adv.* **2014**, *4*, 61343−61354.

(50) Georges, S.; Bria, M.; Zinck, P.; Visseaux, M. Polymyrcene Microstructure revisited from Precise High-Field Nuclear Magnetic Resonance Analysis. *Polymer* **2014**, *55*, 3869−3878.

(51) Lessard, B.; Maric, M. Effect of an Acid Protecting Group on the "Livingness" of Poly(acrylic acid-*ran*-styrene) Random Copolymer Macroinitiators for Nitroxide-Mediated Polymerization of Styrene. *Macromolecules* **2008**, *41*, 7881-7891.

(52) Ma, Q.; Wooley, K. L. The Preparation of *t*-Butyl Acrylate, Methyl Acrylate, and Styrene Block Copolymers by Atom Transfer Radical Polymerization: Precursors to Amphiphilic and Hydrophilic Block Copolymers and Conversion to Complex Nanostructured Materials. *J. Polym. Sci., Part A: Polym. Chem.* **2000**, *38* (S1), 4805-4820.

(53) Glebov, E. M.; Krishtopa, L. G.; Stepanov, V.; Krasnoperov, L. N. Kinetics of a Diels-Alder Reaction of Maleic Anhydride and Isoprene in Supercritical CO_2. *J. Phys. Chem. A* **2001**, *105*, 9427-9435.

(54) Hornung, C. H.; Alvarez-Diéguez, M. A.; Kohl, T. M.; Tsanaktsidis, J. Diels–Alder Reactions of Myrcene using Intensified Continuous-Flow Reactors. *Beilstein J. Org. Chem.* **2017**, *13*, 120-126.

(55) Liu, S.; Srinivasan, S.; Grady, M. C.; Soroush, M.; Rappe, A. M. Backbiting and β-Scission Reactions in Free-Radical Polymerization of Methyl Acrylate. *Int. J. Quant. Chem.* **2014**, *114*, 345-360.

(56) Barth, J.; Buback, M.; Hesse, P.; Sergeeva, T. Termination and Transfer Kinetics of Butyl Acrylate Radical Polymerization Studied via SP-PLP-EPR. *Macromolecules* **2010**, *43*, 4023-4031.

(57) Wenn, B.; Junkers, T. Kilohertz Pulsed-Laser-Polymerization: Simultaneous Determination of Backbiting, Secondary, and Tertiary Radical Propagation Rate Coefficients for *tert*-Butyl Acrylate. *Macromol. Rapid Commun.* **2016**, *37*, 781-787.

(58) Cadova, E.; Dybal, J.; Kriz, J.; Vlcek, P.; Janata, M.; Toman, L. Back-Biting Termination in Methyl Methacrylate/*tert*-Butyl Acrylate Anionic Block Copolymerization. *Macromol. Chem. Phys.* **2008**, *209*, 1657-1665.

(59) Guillaneuf, Y.; Gigmes, D.; Marque, S. R. A.; Astolfi, P.; Greci, L.; Tordo, P.; Bertin, D. First Effective Nitroxide-Mediated Polymerization of Methyl Methacrylate. *Macromolecules* **2007**, *40*, 3108-3114.

(60) Charleux, B.; Nicolas, J.; Guerret, O. Theoretical Expression of the Average Activation− Deactivation Equilibrium Constant in Controlled/Living Free-Radical Copolymerization Operating via Reversible Termination. Application to a Strongly Improved Control in Nitroxide-Mediated Polymerization of Methyl Methacrylate. *Macromolecules* **2005**, *38*, 5485-5492.

(61) Lessard, B.; Ling, E.; Morin, M.; Maric, M. Nitroxide-Mediated Radical Copolymerization of Methyl Methacrylate Controlled with a Minimal Amount of 9-(4-Vinylbenzyl)-9H-carbazole *J. Polym. Sci., Part A: Polym. Chem.* **2011**, *49*, 1033-1045.

(62) Nicolas, J.; Mueller, L.; Dire, C.; Matyjaszewski, K.; Charleux, B. Comprehensive Modeling Study of Nitroxide-Mediated Controlled/Living Radical Copolymerization of Methyl Methacrylate with a Small Amount of Styrene. *Macromolecules* **2009**, *42* (13), 4470-4478.

(63) Dire, C.; Belleney, J.; Nicolas, J.; Bertin, D.; Magnet, S.; Charleux, B. β-Hydrogen Transfer from Poly(methyl methacrylate) Propagating Radicals to the Nitroxide SG1: Analysis of the Chain-End and Determination of the Rate Constant. *J. Polym. Sci., Part A: Polym. Chem.* **2008**, *46* (18), 6333-6345.

(64) Asua, J. M.; Beuermann, S.; Buback, M.; Castignolles, P.; Charleux, B.; Gilbert, R.; Hutchinson, R.; Leiza, J.; Nikitin, A.; Vairon, J.-P.; Herk, A. Critically Evaluated Rate Coefficients for Free-Radical Polymerization, Propagation Rate Coefficient for Butyl Acrylate. *Macromol. Chem. Phys.* **2004**, *205*, 2151-2160.

(65) Contreras-López, D.; Albores-Velasco, M.; Saldivar-Guerra, E. Isoprene (co)Polymers with Glycidyl Methacrylate via Bimolecular and Unimolecular Nitroxide Mediated Radical Polymerization. *J. Appl. Polym. Sci.* **2017**.

DOI: 10.1002/app.45108

(66) Odian, G. Chain Copolymerization. *Principles of Polymerization*, 4th ed.; John Wiley & Sons: Hoboken, NJ, **2004**; 466−505.

(67) Fineman, M.; Ross, S. D. Linear Method for Determining Monomer Reactivity Ratios in Copolymerizations. *J. Polym. Sci.* **1950**, *5* (2), 259−262.

(68) Kelen, T.; Tüdös, F. Analysis of the Linear Methods for Determining Copolymerization Reactivity Ratios. I. A New Improved Linear Graphic Method. *J. Macromol. Sci., Chem.* **1975**, *9* (1), 1−27.

(69) Tidwell, P. W.; Mortimer, G. A. An Improved Method of Calculating Copolymerization Reactivity Ratios. *J. Polym. Sci., Part A: Gen. Pap.* **1965**, *3*, 369−387.

(70) Mayo, F. R.; Lewis, F. M. Copolymerization. I. A Basis for Comparing the Behavior of Monomers in Copolymerization; The Copolymerization of Styrene and Methyl Methacrylate. *J. Am. Chem. Soc.* **1944**, *66* (9), 1594-1601.

(71) Rusakova, K. A.; Kuznetsova, I. M.; Vargasova, N. A.; Margaritova, M. F.; Alekseyeva, S. G.; Urman, Y. G.; Slonim, I. Y. Study of Copolymerization of Isoprene with Glycidyl Methacrylate. *Vysokomol. Soyed.* **1974**, *A16 12*, 2815-2817.

(72) Contreras-López, D.; Saldivar-Guerra, E.; Luna-Barcenas, G. Copolymerization of Isoprene with Polar Vinyl Monomers: Reactivity Ratios, Characterization and Thermal Properties. *Eur. Polym. J.* **2013**, *49*, 1760-1772.

(73) Kamachi, N.; Kajiwara, A. ESR Study on Radical Polymerizations of Diene Compounds. Determination of Propagation Rate Constants. *Macromolecules* **1996**, *29* (7), 2378−2382.

(74) Morton, M.; Salatiello, P. P.; Landfield, H. Absolute Propagation Rates in Emulsion Polymerization. III. Styrene and Isoprene. *J. Polym. Sci.* **1952**, *8* (3), 279−287.

(75) Beuermann, S.; Buback, M.; Davis, T. P.; Garcia, N.; Gilbert, R. G.; Hutchinson, R. A.; Kajiwara, A.; Kamachi, M.; Lacik, I.; Russell, G. T. Critically Evaluated Rate Coefficients for Free-Radical Polymerization. *Macromol. Chem. Phys.* **2003**, *204* (10), 1338-1350.

(76) Liang, K.; Dossi, M.; Moscatelli, D.; Hutchinson, R. A. An Investigation of Free-Radical Copolymerization Propagation Kinetics of Styrene and 2-Hydroxyethyl Methacrylate. *Macromolecules* **2009**, *42*, 7736-7744.

(77) Lessard, B.; Tervo, C.; De Wahl, S.; Clerveaux, F. J.; Tang, K. K.; Yasmine, S.; Andjelic, S.; D'Alessandro, A.; Maric, M. Poly(*tert*-butyl methacrylate/styrene) Macroinitiators as Precursors for Organo- and Water-Soluble Functional Copolymers Using Nitroxide-Mediated Controlled Radical Polymerization. *Macromolecules* **2010**, *43* (2), 868-878.

(78) Gryn'ova, G.; Lin, C. Y.; Coote, M. L. Which Side-Reactions Compromise Nitroxide Mediated Polymerization? *Polym. Chem.* **2013**, *4* (13), 3744−3754.

(79) Runckel, W. J.; Goldblatt, L. A. Inhibition of Myrcene Polymerization during Storage. *Ind. Eng. Chem.* **1946**, *38* (7), 749− 751.

(80) Safa, K. D.; Nasirtabrizi, M. H. Ring Opening Reactions of Glycidyl Methacrylate Copolymers to Introduce Bulky Organosilicon Side Chain Substituents. *Polymer Bulletin* **2006**, *57*, 293-304.

(81) Gordon, M.; Taylor, J. S. Ideal Copolymers and the Second-Order Transitions of Synthetic Rubbers. I. Non-Crystalline Copolymers. *J. Chem. Tech. and Biotech.* **1952**, *2* (9), 493-500.

(82) Fox, T. G. Influence of Diluent and of Copolymer Composition on the Glass Temperature of a Polymer System. *Bull. Am. Phys. Soc.* **1956**, *1*, 123−125.

(83) Dimarzio, E. A.; Gibbs, J. H. Glass Temperature of Copolymers. *J. Polym. Sci., Part A: Polym. Chem.* **1959**, *40* (136), 121-131.

(84) Wood, L. A. Glass Transition Temperatures of Copolymers. *J. Polym. Sci., Part A: Polym. Chem.* **1958**, *28* (117), 319-330.

(85) Orwoll, R. A. Densities, Coefficients of Thermal Expansion, and Compressibilities of Amorphous Polymers. In Physical Properties of Polymers Handbook; Mark, J. E., Ed.; Springer: New York, **2007**; 93-101.

(86) Guseva, D.; Komarov, P.; Lyulin, A. V. Molecular-Dynamics Simulations of Thin Polyisoprene Films Confined Between Amorphous Silica Substrates. *J. Chem. Phy.* **2014**, *140*, 114903-1/14.

(87) Claudy, P.; Létoffé, J. M.; Camberlain, Y.; Pascault, J. P. Glass Transition of Polystyrene Versus Molecular Weight. *Polymer Bulletin* **1983**, *9*, 208-215.

(88) Flory, P. *Principles of Polymer Chemistry*. Ithaca, New York: Cornell University Press; 1975.

(89) Rosenholm, J. B. Solubility and Interaction Parameters as References for Solution Properties. I. Exceptional Mixing and Excess Functions. *Advances in Colloid and Interface Science* **2009**, *146*, 31-41.

(90) Yara-Varon, E.; Fabiano-Tixier, A. S.; Balcells, M.; Canela-Garayoa, R.; Bily, A.; Chemat, F. Is It Possible to Substitute Hexane with Green Solvents for Extraction of Carotenoids? A Theoretical Versus Experimental Solubility Study. *RSC Adv.* **2016**, *6*, 27750-27759.

(91) Hansen, C. M. *Hansen Solubility Parameters, A User's Handbook*, 2nd ed.; CRC Press: New York, **2007**; 1-24.

(92) Manias, E.; Utracki, L. A. Thermodynamics of Polymer Blends. In *Polymer Blends Handbook*; Utracki, L. A., Wilkie, C. A., Eds.; Springer: Dordrecht, **2014**; 171-289.

(93) Higgins, J. S.; Lipson, J. E.; White, R. P. A Simple Approach to Polymer Mixture Miscibility. *Phil. Trans. R. Soc. A* **2010**, *368*, 1009-1025.

(94) Benaglia, M.; Alberti, A.; Giorgini, L.; Magnoni, F.; Tozzi, S. Poly(Glycidyl Methacrylate): a Highly Versatile Polymeric Building Block for Post-Polymerization Modifications. *Polym. Chem.* **2013**, *4*, 124-132.

(95) Mertoglu, M.; Garnier, S.; Laschewsky, A.; Skrabania, K.; Storsberg, J. Stimuli Responsive Amphiphilic Block Copolymers for Aqueous Media Synthesised via Reversible Addition Fragmentation Chain Transfer Polymerisation (RAFT). *Polymer* **2005**, *46* (18), 7726-7740.

(96) Garnier, S.; Laschewsky, A. Synthesis of New Amphiphilic Diblock Copolymers and Their Self-Assembly in Aqueous Solution. *Macromolecules* **2005**, *38* (18), 7580-7592.